

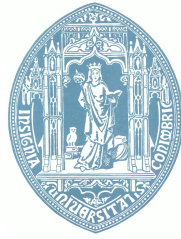
Bruno Miguel da Cruz Lopes

# LED Light Fixtures Efficiency Analysis and Characterization

March 2013



UNIVERSIDADE DE COIMBRA



University of Coimbra  
Faculty of Science and Technology  
Department of Electrical and Computer Engineering

**LED Light Fixtures Efficiency Analysis and Characterization**

Bruno Miguel da Cruz Lopes

Coimbra, 2013

**LED Light Fixtures Efficiency Analysis and Characterization**

**Advisor: PROF. DR. LINO JOSÉ FORTE MARQUES**

Dissertation submitted to obtain the Master degree in Electrical and Computers Engineering

**Jury:**

**President: PROF. DR. PAULO JOSÉ MONTEIRO PEIXOTO**

**PROF. DR. PEDRO MANUEL SOARES MOURA**  
**PROF. DR. LINO JOSÉ FORTE MARQUES**

March 2013

## **Acknowledgments**

Firstly, I would like to express my gratitude to my supervisor Dr. Lino Marques, for all the help and support given throughout the past months.

Next, many thanks to all my friends, which during this course were always there for me, and, particularly during this time:

- Marco Rocha, for his invaluable help with the Goniophotometer construction.
- My colleagues at the Automatic Production Laboratory and Embedded Systems Laboratory: Gilberto Martins, Fábio Faria, Hugo Cura, João Sousa and Jorge Fraga.

Lastly but not least, a really big thanks for my parents, for their belief in me.



## **Abstract**

This work focuses on the luminous efficiency of light fixtures in general and with the LED ones in particular. Applying photometry techniques, a methodology for characterizing light fixtures is outlined and followed.

To achieve this purpose, a single axis goniophotometer is projected, built and demonstrated. Controlling a rotary positioner stage and acquiring measurements from photodiodes using the input analog ports of an Arduino Mega control board, the total luminous flux from a series of representative artificial light sources is calculated in order to quantify how much luminous power was lost in the various modules that compose a light fixture.

**Keywords:** Efficiency, Light, LED, Photodiode, Goniophotometer, Photometry, Luminous Flux

## **Resumo**

Este trabalho incide na eficiência luminosa das luminárias em geral e das LED em particular. Aplicando técnicas da fotometria vai-se desenvolver e seguir uma metodologia de caracterização das luminárias.

Para atingir este objectivo, um luxímetro angular de um único eixo é idealizado, construído e demonstrado. Controlando um posicionador rotativo e adquirindo as medidas dos fotodiodos com um ADC, é calculado o fluxo luminoso total de uma série de fontes de luz artificiais de modo a determinar a potência luminosa perdida nos vários módulos constituintes de uma luminária.

**Palavras-Chave:** Eficiência, Luz, LED, Fotodiodo, Luxímetro Angular, Fotometria, Fluxo Luminoso

# Contents

<b>List of Figures</b>	<b>vii</b>
<b>List of Tables</b>	<b>x</b>
Nomenclature . . . . .	xi
<b>1 Introduction</b>	<b>1</b>
1.1 Objectives of this work . . . . .	1
1.2 Related Work . . . . .	2
1.2.1 Photometry Measurement Techniques and Methodologies . . . . .	2
1.2.2 New ideas to put in practice . . . . .	3
1.3 Dissertation overview . . . . .	4
<b>2 Illumination Concepts</b>	<b>5</b>
2.1 Solid Angle . . . . .	5
2.2 Luminous Flux . . . . .	6
2.3 Illuminance . . . . .	7
2.4 Luminous Intensity . . . . .	8
2.5 Luminance . . . . .	8
2.6 Radiometric Units . . . . .	9
2.7 Luminous Efficacy . . . . .	9
2.7.1 Luminous Efficacy of the Source . . . . .	10
2.7.2 Overall Luminous Efficacy of the Source . . . . .	11
2.7.3 Light Fixture Luminous efficacy . . . . .	11
2.7.4 Light Fixture Efficiency . . . . .	11
2.7.5 Power Efficiency . . . . .	12
2.8 Color Temperature . . . . .	12
2.9 Color Rendering Index . . . . .	13
<b>3 Measurement and Testing Standards</b>	<b>14</b>
3.1 Integrating Sphere . . . . .	15
3.1.1 Operation . . . . .	15
3.2 Goniophotometer . . . . .	16
3.3 Lux Meter . . . . .	17

<b>4</b>	<b>LED Light Fixtures Analysis</b>	<b>18</b>
4.1	LED Module	19
4.1.1	White LED Energy Conversion	20
4.1.2	LED Thermal Runaway	22
4.2	LED Driver	22
4.2.1	Losses in LED Driver	23
4.2.1.1	MOSFETs	24
4.2.1.2	Diodes	24
4.2.1.3	Capacitors	24
4.2.1.4	Magnetic Losses	25
4.3	Fixture	25
4.3.1	Optics	26
4.3.2	Fixture Housing Light Loss	26
4.4	Other Efficiency Losses	27
<b>5</b>	<b>Motivation and Development of Goniophotometer</b>	<b>28</b>
5.1	Mathematical Background	28
5.2	Construction Guidelines	29
5.3	Goniophotometer Control and Data Acquisition	30
5.3.1	National Instruments 6009	30
5.3.2	Arduino Mega	31
5.3.3	Rotary Positioner Micro-Controller	32
<b>6</b>	<b>Error Sources and Calibration</b>	<b>34</b>
6.1	Calibration	35
6.2	Photodiode	36
6.2.1	Reverse Current	36
6.3	Calibration Results	37
<b>7</b>	<b>Experimental Results</b>	<b>39</b>
7.1	Commercial Lamps Testing	39
7.1.1	Light Fixture	40
7.1.2	Results of Lamp Testing	41
7.1.3	Lamps Polar Diagrams and Conclusions	43
7.2	Drivers Testing	45
7.2.1	Driver Testing Results	45
7.3	LED Light Fixture	46
7.3.1	Luminous Efficacy of Source	47
7.3.2	Overall Luminous Efficacy of Source	48
<b>8</b>	<b>Conclusions and Future Work</b>	<b>50</b>

<b>Bibliography</b>	<b>51</b>
<b>A Goniophotometer Construction and Operation</b>	<b>56</b>
A.1 Code developed to operate the Goniophotometer in MATLAB . . . . .	59
A.2 Graphic User Interface . . . . .	64
<b>B Integrating Sphere Theory</b>	<b>66</b>
<b>C Relevant Standards for LED Light</b>	<b>69</b>
C.1 Performance . . . . .	69
C.2 Electromagnetic Compability . . . . .	69
C.3 Funcionality . . . . .	69
C.4 Security . . . . .	69

# List of Figures

- 2.1 Electromagnetic radiation.
  - Left: Response of the human eye under photopic and scotopic conditions.
  - Right: Electromagnetic spectrum (of all kinds). . . . . 5
- 2.2 Solid angle illustrations.
  - Left: Illustration of the relation between solid angle, radius and surface.
  - Right: Analogy between a 2D angle and 3D angle. . . . . 6
- 2.3 Illuminance properties.
  - Left: Inverse square law.
  - Right: Angular displacement intensity response of a photometer. . . . . 7
- 2.4 Luminous Intensity. . . . . 8
- 2.5 Luminance and projected area. . . . . 9
  
- 3.1 Integrating sphere.
  - Left: Typical design.
  - Right: Illustration depicting the beam reflections inside the sphere. . . . . 15
- 3.2 Goniophotometer.
  - Left: An example of a goniophotometer.
  - Right: A possible goniophotometer operation illustration. . . . . 16
- 3.3 ISO-TECH ILM350 used in the laboratory. . . . . 17
  
- 4.1 Led Light.
  - Left: LED color wavelenght generation.
  - Right: Typical spectrum of “white” light created by mixing the output of red, green, and blue monochromatic LEDs. Relative intensity is represented in arbitrary units. . . . . 20
- 4.2 LED’s in detail.
  - Left: Close up of the high power LED’s present on the ARQULED strings.
  - Right: Typical composition of a LED for lighting purposes. . . . . 20
- 4.3 Spectral radiance of a black body. Energy outside the visible wavelength range (~380–750 nm, shown by grey dotted lines) reduces the luminous efficiency. . . . . 21
- 4.4 Common LED driver topologies.
  - Top: Buck converter (non-isolated).
  - Bottom: Flyback converter. . . . . 23

4.5	MOSFET and diode waveforms. Left: MOSFET losses. Right: Diode losses. . . . .	25
4.6	Some types of LED optical designs. Left: LED bulb. Center: LED light fixture for use in public lighting. Right: LED lamp with minimal lumen output loss due to its conical form. . . . .	26
4.7	Losses within the fixture in two different cases. . . . .	26
5.1	Scanning sphere referencial. . . . .	30
5.2	Goniophotometer built for the project. . . . . .	30
5.3	Goniophotometer control diagram. . . . .	31
5.4	Photodiode measurements. Left: Aquisition board NI-6009 used as ADC. Right: NI-6009 used in photodiode calibration. . . . .	31
5.5	Arduino Mega. Left: Arduino Mega microcontroller board. Right: Setup to aquire the photodiode measurements. . . . .	32
5.6	Rotary positioner control. Left: UR80 stage and UE-31-PP motor ftom Micro-Controle. Right: Technosoft IDM640-8EI Driver. . . . .	33
6.1	BPW34 Photodiode. Left: Angular displacement. Right: Spectral response. . . . .	35
6.2	Spectral response of cool white LEDs . . . . .	36
6.3	Photodiode measurements. Left: Measurement circuit for photodiode mode. Right: I-V curve of a photodiode and the equivalent circuit. The linear load lines represent the response of the external circuit. The points of intersection with the curves represent the actual current and voltage for a given bias, resistance and illumination. . . . .	37
6.4	Illuminance relation with the distance to luminous source (the LED string). . . . .	38
7.1	Light fixture used to accomodate the lamps. . . . .	40
7.2	Sphere discretization obtained with 20 slices and a fixed displacement of 9 degrees between the photodiodes. . . . .	41
7.3	Lamp Testing. Left: Compact Fluorescent Lamp (CFL). Right: LED Lamp. . . . .	42
7.4	Lamps efficacy chart. . . . .	43

- 7.5 LED lamp polar diagrams.
  - Left: Polar diagram in plane  $\theta = 0^\circ$ .
  - Right: Polar diagram in plane  $\varphi = 90^\circ$ . . . . . 44
- 7.6 CFL lamp polar diagrams.
  - Left: Polar diagram in plane  $\theta = 0^\circ$ .
  - Right: Polar diagram in plane  $\varphi = 90^\circ$ . . . . . 44
- 7.7 Configuration for RECOM Driver with 2 strings, with output current at 700 mA. 45
- 7.8 Configuration for JRLED Driver. . . . . 45
- 7.9 LED lamp opened.
  - Left: SMD LEDs exposed.
  - Right: Driver. . . . . 46
- 7.10 Setup for the JRLED photometry test. . . . . 46
- 7.11 Polar diagrams of the JRLED test.
  - Left: Left: Polar diagram in plane  $\theta = 0^\circ$ .
  - Right: Polar diagram in plane  $\varphi = 90^\circ$ . . . . . 47
- 7.12 Luminous efficacy losses of LED Light Fixture . . . . . 47
- 7.13 Luminous total power loss of the LED lamp inserted in light fixture, considering a luminous efficiency of a “ideal white source” (37%). . . . . 49
  
- A.1 Photodiodes incorporation on arc.
  - Left: Top view of the photodiodes inserted on rubber, to fit in the rim holes.
  - Right: Photodiodes connected to cables. . . . . 56
- A.2 Rotary positioner stage.
  - Left: External view.
  - Right: Internal view. . . . . 57
- A.3 Goniophotometer after completion. . . . . 57
- A.4 Goniophotometer dimensions. . . . . 58
- A.5 Developed GUI for the goniophotometer. . . . . 65



# List of Tables

2.1	Radiometric and Photometric quantities. . . . .	9
2.2	Examples of Color Temperature and CRI. . . . .	13
3.1	Types of measurement in photometry. . . . .	14
3.2	Standards to regulate photometry measurements and LED light fixture's testing. . . . .	14
5.1	Arduino ATmega1280 characteristics. . . . .	32
5.2	UR 80 Stage characteristics . . . . .	33
6.1	Calibration measures using a LED string with 9 LEDs. . . . .	37
6.2	Calibration constants for the various light sources. . . . .	37
7.1	Various types of lamps to be tested. . . . .	40
7.2	Results of lamp testing. . . . .	42
7.3	Specifications given by the manufacturers of the drivers available for test. . . . .	45
7.4	Measurements made to the drivers with the power analyzer. . . . .	46
C.1	Standards related to performance . . . . .	69
C.2	Standards related to EMC . . . . .	70
C.3	Standards related to functionality . . . . .	70
C.4	Standards related to security . . . . .	70

# Nomenclature

LED	Light-Emitting Diode
ILB	Incandescent Light Bulb
CFL	Compact Fluorescent Lamp
SMD	Surface-Mount Device
SMPS	Switched-Mode Power Supply
CT	Colour Temperature (K)
CRI	Colour Rendering Index
DC	Direct Current
ADC	Analog to Digital Converter
ESR	Effective Series Resistance
$V(\lambda)$	Photometric Distribution
$\lambda$	Wavelength (m)
$V_f$	LED Forward Voltage
$R_{DS(ON)}$	MOSFET saturation resistance ( $\Omega$ )
P	Electrical Power (W)
I	Current (A)
$C_{PH}$	Calibration Constant
$K_{PH}$	Photodiode Constant
A	Area ( $m^2$ )
R	Electrical Resistance ( $\Omega$ )
AC	Alternating Current

V	Voltage (V)
l	length (m)
r	Radius (m)
$\alpha$	Plane Angle (rad)
$\Omega$	Solid Angle (sr)
$\vec{d}$	Direction Vector
$\vec{n}$	Normal Vector
$\Phi_V$	Luminous Flux (lm)
$\Phi_E$	Radian Flux (W)
$\rho_E$	Luminous Efficacy of Radiation ( $lm/W$ )
$I_V$	Luminous intensity (cd)
$\eta_E$	Radiant Efficiency of the Source
$E_V$	Illuminance (lx)
$L_V$	Luminance ( $cd/m^2$ )

# Chapter 1

## Introduction

Energy saving is not only a major driving force in today's global crisis of costly energy trends, but also an opportunity for new technologies to pave the way. LED lighting is one of those technologies. Long life, energy efficiency, design flexibility and light quality are key advantages of LED lighting,

An important reason for LED light adoption is the importance of increasing the efficiency of public lighting on streets and cities. Traditional street lamps require extremely high power to generate light, and the LED light technology will play an important role on reducing energy costs.

It's important the study of LED light fixtures to know where the efficiency can be improved. For that objective to be fulfilled it's important, first of all, to understand how light is measured and perceived by the human eye so a broad sense of efficiency is achieved.

### 1.1 Objectives of this work

The goal of this thesis is to measure the efficiency of LED light fixtures and identify the losses in each element. To achieve this goal a low cost goniophotometer was built, and lamps and LED drivers were tested in both photometric and electrical consumption ways.

So, the main goals of this dissertation can be summarized as follow:

- To study in detail the light photometry theory and how it can be applied on the evaluation of LED light fixtures.
- To identify and study the methods and standards on how light fixtures are characterized.
- To use the photometry theory to calculate the total luminous flux emitted by a light source.
- To compare some commercial light fixtures using different types of lamps, LED ones and of other types (ILB, CFL and Halogen) on a light fixture in terms of luminous efficiency.
- To test various LED Drivers to evaluate energy efficiency.

## 1.2 Related Work

Bellow are summarized some of the related work and research that was done regarding photometry measurement techniques and also LED light fixtures efficiency.

### 1.2.1 Photometry Measurement Techniques and Methodologies

In 1998:

- [1] Apina-Bennewitz et al. improved a device for measuring light distribution, a goniophotometer, with new detector geometry and faster data acquisition. The integration method used Voronoi cells on a sphere to integrate arbitrarily located data points, using adaptively refined angular resolution of the measured scattering data. This links the bidirectional-reflection-transmission-function (BRDF) of goniophotometers with the direct-hemispherical transmittance values typically given by integrating spheres.
- [2] Fiorentin et al. presented two methods for the measurement of the luminous flux. The first is based on an integrating sphere and a luminous flux standard lamp, the second utilizes an accurate goniophotometer. A comparison between the two methods is carried on for two different light sources: an LED and a halogen source, presenting different luminous fluxes. The measuring procedure and an evaluation of the measurement uncertainties are described for both the methods.
- [3] Fiorentin et al. constructed an accurate goniometer, being a part of a system that is designed for the measurement of reflecting properties of surfaces. It can be used to orient a surface of the sample under test arbitrarily with respect to the observing direction and the direction of the shooting light beam. The high performance (revolution angle uncertainty equal to  $0.1^\circ$ , which is required as a specification for the construction, is checked. Particular attention has been given to analyzing the orthogonality among the revolution axes of each goniometer component and their convergence in the goniometer center. The linearity error of each revolution motion has been measured by using a differential method, which proves to be effective in highlighting the small linearity deviation and verifying the uncertainty declared by the manufacturer.

In 2009:

- [4] Dias et al. presented the practical implementation details of a simplified and low cost technique useful to provide elements that sustain the comparison between conventional small size, low wattage lamps (or luminaires) and LED-based modern counterparts. A case study was also included, which consisted of the comparison of a high-power LED linear light fixture, composed of four LEDs of 3W in series, with a conventional 15W fluorescent bulb, which was fed by an electronic ballast. The LED luminaire implementation was also described in the text, along with some details of the power driver design. Experimental results, assembling electrical and luminous parameter

information (illuminance), were also given, revealing that the simple LED arrangement could easily overcome the performance of the fluorescent bulb.

In 2010:

- [5] Apian-Bennwitz proposed a new design of a scanning, out of plane goniophotometer with optimised mechanical electronic design, reduced scanning time and optimised sensors resulting in high dynamic range, low noise and extended measurement capabilities.
- [6] Poikonen et al. projected a multifunctional setup, based on the absolute integrating-sphere method, for measuring luminous flux of LEDs. The setup consists of a 30 cm integrating sphere, a standard photometer with a closely cosinoidal angular response, temperature stabilizers for both LP and HP-LEDs, and a temperature controller unit. The total luminous flux in 2 and 4 geometries and the partial luminous flux with variable aperture angle can be measured with the same custom-made integrating sphere.

In 2011:

- [7] Sametoglu et al. constructed a two-axis goniophotometer for characterizing photometric properties of compact light sources. With this new device, total luminous flux emitted by a light source at both cap-up or cap-down mounting positions is calculated from the integration of the illuminance values  $E_V(\theta; \varphi)$  measured on the goniometric spherical surface. The internal calibration of the system is performed by means of two calibrated light sources with known luminous flux values. The constructed system is also capable of measuring the luminous intensity distribution values  $I_V(\theta; \varphi)$  of compact light sources. The uncertainty analysis of the luminous flux measurements as well as the internal calibration of the instrument are also presented.
- [8] Tetervenoks et al. developed an evaluation stand to ensure optical and electrical parameter simultaneous measurements. The illumination parameter measurement process was automatic to speed up the analysis for different lighting device calculations. The stand was suitable for preliminary testing of developed luminaries, existing products and analyzing data to evaluate lighting dimming process efficiency at different dimming levels.

### 1.2.2 New ideas to put in practice

Since the integrative sphere is an expensive device, to acquire the total flux measurements in a practical and functional way, a single axis goniophotometer will be constructed. With this prototype, the artificial light source will be placed in the center. The total luminous flux will be calculated from the integration of the illuminance values  $E_V(\theta, \varphi)$ , measured on the virtual spherical surface.

The rotation of the arc (a section of a bicycle rim) containing the photodiodes will be achieved using a rotary positioner. With this device the creation of polar diagrams showing the luminous intensity distribution is possible .

A graphical interface will be created so the user can adjust various parameters of the setup and data representation.

### 1.3 Dissertation overview

The dissertation is organised as follows:

- Chapter 1 - Briefly introduction to the theme of the thesis, proposed objectives and the chapter structure;
- Chapter 2 - Exposition of the related works in the luminous flux measurements and LED light fixtures analysis;
- Chapter 3 - Explanation of the principal concepts of photometry;
- Chapter 4 - Description a LED Light Fixture and identification of the main loss mechanisms present in each module;
- Chapter 5 - Justify the project of a goniophotometer in terms of luminous flux measurement and describe his characteristics;
- Chapter 6 - Identify the sources of errors in the measurements taken;
- Chapter 7 - Explain the calibration process and presentation of the calibration data;
- Chapter 8 - Demonstrate the goniophotometer utilization to characterize a LED light fixture (by itself or in modules);
- Chapter 9 - Conclusions.

For structure reasons, some non-essential of parts of this dissertation and accessory information were omitted from the main text and included in appendices.

# Chapter 2

## Illumination Concepts

Photometry is the science of the measurement of light, in terms of how its brightness is perceived by the human eye. It is distinct from radiometry, which consists of measuring the radiant energy (including light) in terms of absolute power (Fig. 2.1, right). In photometry, the radiant power on each wavelength is weighted by a luminosity function that models human brightness sensitivity (Fig. 2.1, left).

This is a standardized function which represents the response of a "typical" eye under photopic vision (well lit conditions). One can also define a similar curve for scotopic vision (dim conditions). When neither is specified, photopic conditions are generally assumed.

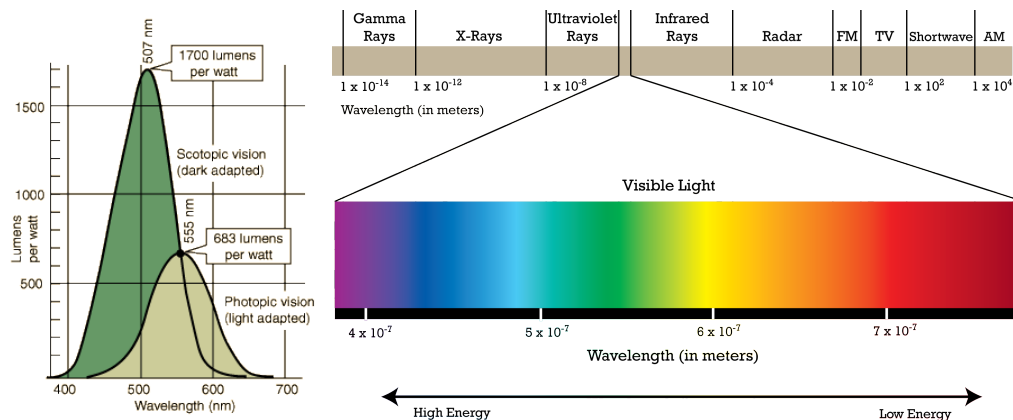


**Figure 2.1:** Electromagnetic radiation.

Left: Response of the human eye under photopic and scotopic conditions [9].

Right: Electromagnetic spectrum (of all kinds) [10].

### 2.1 Solid Angle

The geometrical configurations of luminous intensity and illuminance use the 3D concept of a solid angle, which is analogous to the 2-dimensional plane angle,  $\alpha$ . In Fig. 2.2,  $l$  is the arc length subtended by the limits of the 2D object at the center of the circle of radius  $r$ . The definition of the plane angle  $\alpha$  is given by:



$$\alpha = \frac{l}{r} \quad (2.1)$$

The SI unit for the plane angle is the radian, rad. A full circle has an angle of  $2\pi$  rad.

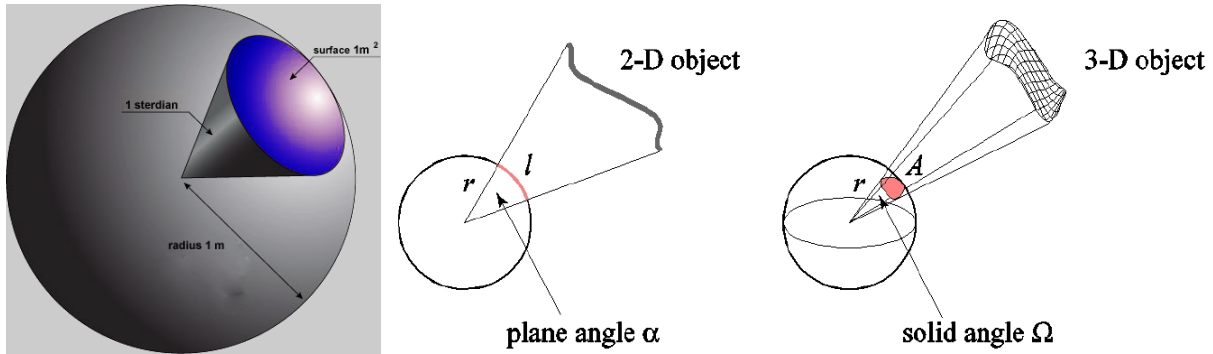


**Figure 2.2:** Solid angle illustrations.

Left: Illustration of the relation between solid angle, radius and surface [11].

Right: Analogy between a 2D angle and 3D angle [12].

Much in the same way, in the 3D angle, called a solid angle,  $A$  is the area of the part of the  $r$  radius sphere subtended by the limits of the 3D object at the center of a sphere. The definition of the solid angle,  $\Omega$ , is given by:

$$\Omega = \frac{A}{r^2} \quad (2.2)$$

The SI unit for the solid angle is called the steradian, sr. The complete sphere has a solid angle of  $4\pi$  sr.<sup>1</sup>

Placing a punctual light source with a luminous intensity of 1 candela at the centre of the sphere, and measuring the light being emitted into one steradian, we get 1 lumen.

## 2.2 Luminous Flux

In photometry, luminous flux or luminous power is the measure of the perceived power of light. It differs from radiant flux, the measure of the total power of light emitted, in which luminous flux is adjusted to reflect the varying sensitivity of the human eye to different wavelengths of light.

The SI unit of luminous flux is the lumen (lm). One lumen is defined as the luminous flux of light produced by a light source that emits one candela of luminous intensity over a solid angle of one steradian. In other systems of units, luminous flux may be expressed in units of power.

The total luminous flux in lumens of a light source is obtained, multiplying the intensity (in candelas) by the angular span over which the light is emitted. With the symbol  $\Phi_V$  for

<sup>1</sup>Because the surface area of a sphere is  $4 \cdot \pi \cdot r^2$ , the definition of solid angle implies that a sphere measures  $4 \cdot \pi \approx 12,56637$  sr. Analogously, the maximum solid angle that can be subtended at any point is  $4 \cdot \pi$  sr.

lumens,  $I_V$  for candelas and  $\Omega$  for the angular span in steradian, the relation is:

$$\Phi_V = I_V \cdot \Omega \quad (2.3)$$

If a light source is isotropic (uniform in all directions),  $\Phi_V = 4\pi \cdot I_V$ . This is because a sphere measures  $4\pi$  steradians.

## 2.3 Illuminance

The illuminance is the amount of visible light reaching a given point on a defined surface area (i.e. the luminous flux). Illuminance is measured in lux (lx), and its measurement will include all light that reaches that point, from a  $180^\circ$  hemisphere. It is related to the luminous flux by:

$$1\text{lx} = 1\text{lm}/\text{m}^2 \quad (2.4)$$

Luminous emittance is the luminous flux per unit area emitted from a surface.

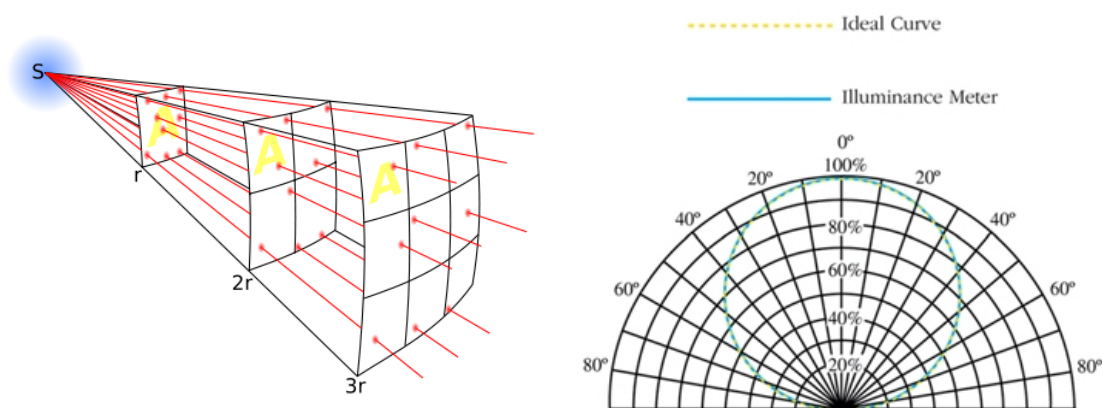


**Figure 2.3:** Illuminance properties.

Left: Inverse square law [13].

Right: Angular displacement intensity response of a photometer [14].

The distance between a surface and the source affects the illuminance (luminous flux per unit of area) striking that surface. Surface of a given area, closer to the source, captures a larger portion of the flux than a surface of the same given area further away, as it can be illustrated on Fig. 2.3 (left).

Considering the luminous intensity as the luminous flux leaving a source in a specific solid angle, as the area increases the illuminance decreases while the luminous flux remains the same.

Inverse square law states that the cross-sectional area of the spherical surface increases with the square of the distance from the source. Therefore, the illuminance on this surface decreases in proportion to the square of the distance from the source.

Surface orientation is included in the inverse square law by adding a  $\cos(\theta)$  term.  $\theta$  is the angle between the light ray coming from the source to the point, and a line that is

perpendicular (normal) to the plane or surface on which the illuminance is being measured or calculated (Fig. 2.3, right). The cosine response of a photometer is given as following:

$$E_V = \frac{I_V}{d^2} \cdot \cos(\theta) \quad (2.5)$$

## 2.4 Luminous Intensity

To define the luminous intensity, one must indicate the direction from the source,  $\vec{d}$ , in which the intensity is to be defined (Fig. 2.4). Then, the intensity of the source, in this specified direction, is defined as the ratio of the flux,  $\Phi_V$ , propagating into an element of solid angle,  $\Omega$ , containing that specified direction, divided by the size of that element of solid angle. The luminous intensity,  $I_V$ , is defined as:

$$I_V = \frac{\Phi_V}{\Omega} \quad (2.6)$$

with SI unit of candela (cd).  $1\text{cd} = 1\text{lm}/\text{sr}$ .

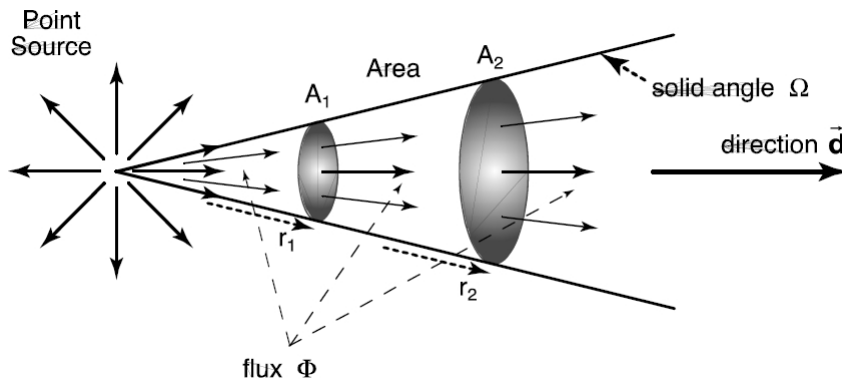


Figure 2.4: Luminous Intensity [12].

## 2.5 Luminance

Luminance, is photometrically weighted radiance. In terms of visual perception, the human eye perceives luminance.

It takes into account that a radiation source is not a point, but an extended surface, and that a radiation source does not emit the same flux into all directions. Therefore there is a quantity that specifies the flux,  $\Phi_V$ , emitted by a radiation surface from a specified area,  $A$ , on the surface and in a specified direction,  $\vec{d}$ , from the surface, and striking a specified solid angle,  $\Omega$ , containing the given direction,  $\vec{d}$ .

The vector direction,  $\vec{n}$ , is the perpendicular to the radiation source element of area  $A$ , and  $\alpha$  is the angle between  $\vec{n}$  and  $\vec{d}$ . On Fig. 2.5 is depicted the relation between the surface of luminous source and the projected area.

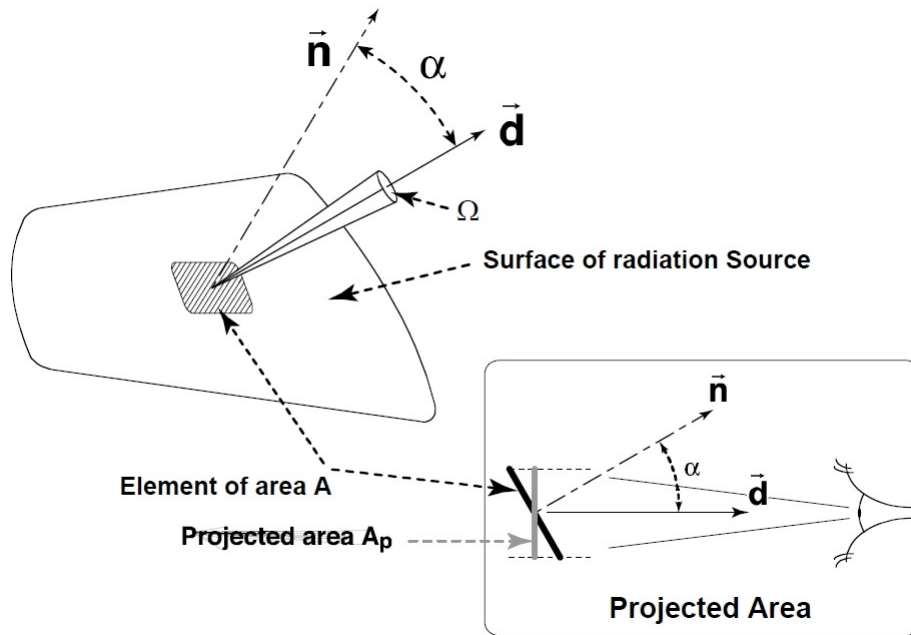


Figure 2.5: Luminance and projected area [12].

The candela per square metre ( $\text{cd}/\text{m}^2$ ) is the derived SI unit of luminance. The unit is based on the candela, the SI unit of luminous intensity, and the square metre, the SI unit of area. Nit (nt) is a non-SI designation, but often used ( $1\text{nit} = 1\text{cd}/\text{m}^2 = \text{lm}/(\text{m}^2 \cdot \text{sr})$ ).

## 2.6 Radiometric Units

Radiometry has a set of quantities and units in analogous to those of the photometry. However his domain encompasses the visible and non-visible electromagnetic spectrum of the light. In Table 2.1 are described the quantities in both domains.

	Radiometric	Photometric
Flux	Radiant Flux W	Luminous Flux lm
Flux/Area	Irradiance $\text{W}/\text{m}^2$	Illuminance $\text{lux}=\text{lm}/\text{m}^2$
Flux/Solid Angle	Radiant Intensity $\text{W}/\text{sr}$	Luminous Intensity $\text{candela}=\text{lm}/\text{sr}$
Flux(Area · Solid Angle)	Radiance $\text{W}/(\text{m}^2 \cdot \text{sr})$	Luminance $\text{nit}=\text{lm}/(\text{m}^2 \cdot \text{sr})$

Table 2.1: Radiometric and Photometric quantities.

## 2.7 Luminous Efficacy

Luminous efficacy is a measure of how well a light source produces visible light. It is the ratio of luminous flux to power. The power can be either the radiant flux of the source's

output, or it can be the total power (electric power, chemical energy, or others) consumed by the source.

Normally when luminous efficacy is referred is the luminous efficacy of the source, but this must be inferred from the context.

### 2.7.1 Luminous Efficacy of the Source

The energy efficiency<sup>2</sup> of a light source is evaluated by luminous efficacy of a source (often called simply “luminous efficacy”), which is the ratio of luminous flux (lumen) emitted by the source to the input electrical power (watt). The luminous efficacy of a source,  $\rho_V$  (lm/W), is determined by two factors:<sup>3</sup>

$$\rho_V = \eta_E \cdot \rho_E \quad (2.7)$$

- where  $\eta_E$  is the radiant efficiency of the source (output radiant flux to input electrical power). “External quantum efficiency” [15] is often used in the same meaning).

$$\eta_E = \frac{\Phi_E}{P_{IN}} \quad (2.8)$$

$\Phi_E$  is the radiant flux or radiant power. Is the measure of the total power of electromagnetic radiation (including infrared, ultraviolet, and visible light). The power may be the total emitted from a source, or the total landing on a particular surface. His unit is the watt (W).

- $\rho_E$  is the luminous efficacy of radiation (ratio of luminous flux to radiant flux)<sup>4</sup>, and is determined by the spectral distribution  $S(\lambda)$  of the source as given by:

$$\rho_E = \frac{K_m \cdot \int_{\lambda} V(\lambda) S(\lambda) d\lambda}{\int_{\lambda} S(\lambda) d\lambda} \quad (2.9)$$

where  $K_m = 683 \text{ lm/W}$ , the maximum possible efficacy corresponding to a wavelength of 555 nm.

The fraction:

$$V_{COEF} = \frac{\int_{\lambda} V(\lambda) S(\lambda) d\lambda}{\int_{\lambda} S(\lambda) d\lambda} \quad (2.10)$$

It's called luminous coefficient,  $V_{COEF}$ , and is unity for the said 555 nm wavelength.

$V(\lambda)$  is the photometric distribution. In the photopic case, outside the 360-830nm range  $V(\lambda)$  is exactly zero.<sup>5</sup>

<sup>2</sup>In lighting, we are concerned with the amount of light (in lumens) produced by a certain amount of electricity (in watts). The term “efficiency” usually is dimensionless. Thus, the term “efficacy” is used, as normally it is used, where the input and output units differ.

<sup>3</sup>On this equation the  $\rho_E$  is normally designated by the  $K$  letter, however this would cause some confusion with other definitions in this work, and it was choosed the use of  $\rho_E$  to denote the luminous efficacy of radiation.

<sup>4</sup>It is also known as LER.

<sup>5</sup>In the scotopic case  $V(\lambda)$  is zero outside the 360-640 nm and  $K_m = [1700] \text{ lm/W}$  corresponding to a wavelength of 507 nm.

As the luminous efficacy of radiation can be expressed simply by:

$$\rho_E = \frac{\Phi_V}{\Phi_E} \quad (2.11)$$

Substituting equations 2.11 and 2.8 in equation 2.7 yields:

$$\rho_V = \frac{\Phi_V}{P_{IN}} \quad (2.12)$$

6

## 2.7.2 Overall Luminous Efficacy of the Source

The overall luminous efficacy of a source is more analytic indicator. It is the product of two factors:

Efficiency of the source energy conversion to electromagnetic radiation

Efficiency of the emitted radiation in being detected by the human eye. It can be formulated as:

$$\rho_{V_{OVERALL}} = \frac{\Phi_V}{P_{IN}} \cdot V_{COEFF}$$

## 2.7.3 Light Fixture Luminous efficacy

Light fixture efficacy describes the efficacy of the entire light fixture, including the light source and optical losses in the transmissive form and reflective form.

$$\rho_{VFIX} = \frac{\Phi_{OUT}}{P_{IN}} \quad (2.13)$$

It is expressed in lumens per Watt (ratio of useful luminous flux to electrical power absorbed by the source from the electrical grid).

## 2.7.4 Light Fixture Efficiency

Light fixture efficiency,  $\eta_{FIX}$ , is the ratio between the light output emitted by the fixture,  $\Phi_{OUT}$  and the nominal light output emitted by its lamps,  $\Phi_N$ . Another way of looking at it: Fixture efficiency is the percentage of light output produced by the LEDs or lamps, that are in turn emitted by the fixture.

$$\eta_{FIX} = \frac{\Phi_{OUT}}{\Phi_N} \quad (2.14)$$

Not all light produced by lamps exit the fixture; some of course remains trapped inside and dissipates as heat. The fixture's physical characteristics will affect the amount of light that exits and how much of that is directed towards the workplane. Light fixture efficiency is

---

<sup>6</sup>While various definitions are used in the LED industry, those introduced above are the most commonly used internationally [16].

important because since one can have a very efficient lamp-ballast system, but as long as the fixture itself is not efficient at delivering lumens, then the lighting system overall will neither be.

Factors that affect the efficiency of the light fixture include its shape, the reflectance of its materials, how many lamps are inside the housing (and how close they are to each other), and whether shielding material such as a lens or louver is used to soften or scatter the light [17].

While a high level of light fixture efficiency should be evaluated, overemphasizing it, of course, can lead to poor lighting quality, because of glare effects and lack of directionality. A good light fixture must have a high efficacy in terms of lumen output but also have a good lighting quality.

### 2.7.5 Power Efficiency

To convert the usual AC electrical power in DC power, a driver is necessary. Electrical losses occur in that process, and therefore some luminous output losses occur as well. To feed a LED string with a nominal power,  $P_N$ , losses will occur in the supplied power,  $P_{IN}$ .

$$\eta_{DRV} = \frac{P_N}{P_{IN}} \quad (2.15)$$

The LED driving electronics convert the available power source (e.g., wall-plug AC or battery) to a stable current source. Just as with any power supply, this process is not 100% efficient. The electrical losses in the driver decrease the overall luminaire efficacy by wasting input power on heat instead of light. The electrical loss should be taken into account when designing the LED system. Typical LED drivers have efficiencies between 80 and 90 percent. Drivers with efficiency over 90 percent will have much higher costs.

## 2.8 Color Temperature

Color temperature is based on the wavelength of light emitted by a material when it is heated. By definition, if a light source is said to be 5500 Kelvin (K), it emits the same wavelength of light, and the same color of light, as if it was a perfect black body radiator heated to 5500 Kelvin. A black body radiator is a theoretical material that absorbs 100 percent of the radiation that strikes it when the body is at absolute zero ( $-273$  °C).

Although there are no true black bodies in the real world, graphite and various metals have a very close behaviour. In the original experiments by William Kelvin (1824–1907), a block of heated carbon was used. The Kelvin measurement only refers to the thermal temperature of the theoretical black body radiator and is not the actual temperature of a light source. In other words, a fluorescent lightbulb does not have to reach a real 4000K to produce the same color of light as the black body radiator at 4000K. Instead, the color of the bulb is roughly correlated to the color of the heated black body.

## 2.9 Color Rendering Index

The color rendering index (CRI), sometimes called color rendition index, is a quantitative measure of the ability of a light source to reproduce the colors of various objects faithfully in comparison with an ideal or natural light source. Light sources with a high CRI are desirable in color-critical applications such as photography and cinematography.

CRI's ability to predict color appearance has been criticized in favor of measures based on color appearance models, such as CIECAM02 and, for daylight simulators, the CIE Metamerism Index [18]. CRI is not a good indicator for use in visual assessment, especially for sources below 5000 kelvin [19].

A newer version of the CRI, R96a, has been developed, but it has not replaced the better-known  $R_a$  general color rendering index [20].

On Table 2.2, the color temperature of various light sources are seen, with the associated CRI.

Light Source	Color Temperature [K]	Color Rendering Index (Ra)
Candle	1700	100
High Pressure Sodium	2100	25
Incandescent	2700	100
Tungsten Halogen	3200	95
Cool White	4200	62
Clear Metal Halide	5500	60
Natural Sunlight	5000-6000	100
Daylight Bulb	6400	80

**Table 2.2:** Examples of Color Temperature and CRI.



# Chapter 3

## Measurement and Testing Standards

Dependig on how the electromagnetic radiation is to be measured, one can use different techniques. In photometry, there are 4 types of possible measurements showed on Table 3.1:

Type	Light emmited	Measure	Unit
Total flux	in all directions	Total luminous flux	lm
Angular intensity	in specified directions and angles	Luminous Intensity	cd=lm/sr
At a surface	in specified directions and angles	Illuminance	lx=lm/m <sup>2</sup>
At the source	from areas within the source	Luminance	cd/m <sup>2</sup> =lm/(sr · m <sup>2</sup> )

**Table 3.1:** Types of measurement in photometry.

Several international organizations regulate the methods to measure the various light quantities. On Table 3.2 are listed the most relevant standards related and the corresponding photometry measurement techniques.

Standard	Date	Description
EN 60598-1	Sep 2006	Luminaires - General Requirements and Tests
IEC 60838-2-2	May 2006	Miscellaneous Lampholders - Particular Requirements Connector for LED Modules
IEC PAS 62717	Apr 2011	LED Modules for General Lighting Performance Requirements
IESNA-LM-79-08	Jan 2008	Electrical and Photometric Measurements of Solid-State Lighting Products
CIE 127 2nd ed.	2007	Measurement of LEDs

**Table 3.2:** Standards to regulate photometry measurements and LED light fixture's testing.

On this work, these standards are taken in account as guidelines, although for some particular specifity or requirement they were not strictly followed due to the limitations inherent of a work of this scope.

## 3.1 Integrating Sphere

Industrially, the measurement of the luminous flux is done according to DIN 5032 section 1 and CIE Publication No. 84 "The Measurement of Luminous Flux". Normally that implies the use of an integrating sphere, a device that, like the name implies, reflects all the luminous flux to one point, integrating all the luminous flux emitted by the luminous source.

In an integrating sphere the detected flux is always a small fraction of the incident flux. This attenuation, caused by light reflecting many times before reaching the detector, makes the integrating sphere ideal for measurement the output power of high-power light sources.

### 3.1.1 Operation

An integrating sphere (also called Ulbricht sphere) is an optical device for various purposes such as measuring the optical flux from a laser diode, light-emitting diode (LED) or bulb, or measuring scattering losses from a surface. It is a hollow sphere with a diffusely reflecting internal surface, typically two or more small openings (ports) for introducing light or attaching a photodetector, and often some so-called baffles or suppressors, which are light barriers used to prevent direct illumination of a detector by a light source. A typical integrating sphere setup and the reflections occurring on its interior surface, are depicted on Fig. 3.1.

The arrangement causes many diffuse reflections of the introduced light before it reaches a detector, so that the light flux becomes very uniform at the detector, and nearly independent of the spatial and polarization properties of the introduced light. The detected optical power depends only on the total introduced power. In that way, the total output power of a laser diode can be measured, even if the beam divergence is fairly large [21].

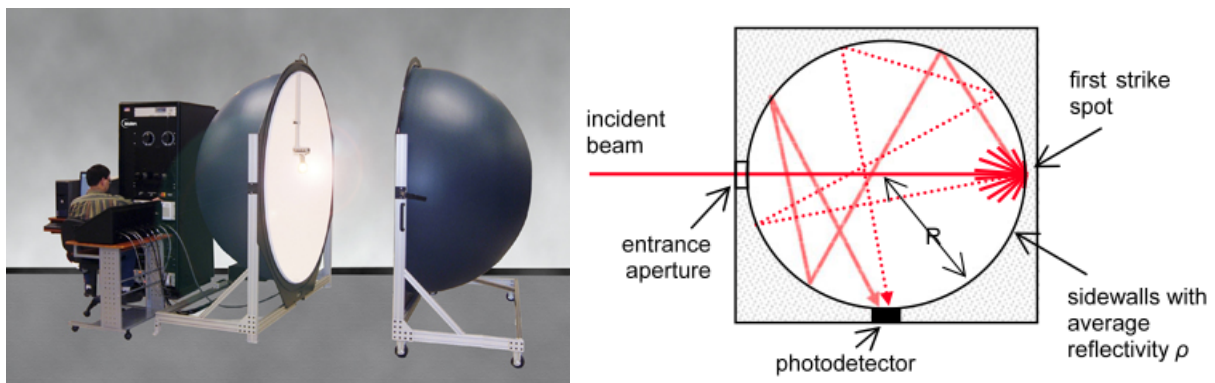


**Figure 3.1:** Integrating sphere.

Left: Typical design [22].

Right: Illustration depicting the beam reflections inside the sphere [23].

Ideally, the coating on the inner side of the integrating sphere has a very high reflectivity over the required wavelength range, and the reflection is very diffuse. If the optical losses in the sphere and through the small ports are low, the multiple reflections can lead to a fairly high optical intensity inside the sphere and consequently to a high optical efficiency, even if

the sphere is much larger than the light source and the detector.

It has the advantage over a goniophotometer for measuring the light produced by a source, because the total power can be obtained in a single measurement. However his cost is high.

## 3.2 Goniophotometer

This device results of two concepts working together, the Goniometer (angular measurement instrument, the word gonio ( $\gamma\omicron\nu\iota\omicron$ ) derives from the Greek meaning angle) and the Photometer (derives from the Greek photon ( $\varphi\omicron\tau\omicron\nu$ ), light measurement device).

This device was designed primarily for measuring luminous intensity, and there are various methods of construction, with one or more independent rotational axis, as shown on Fig. 3.2.

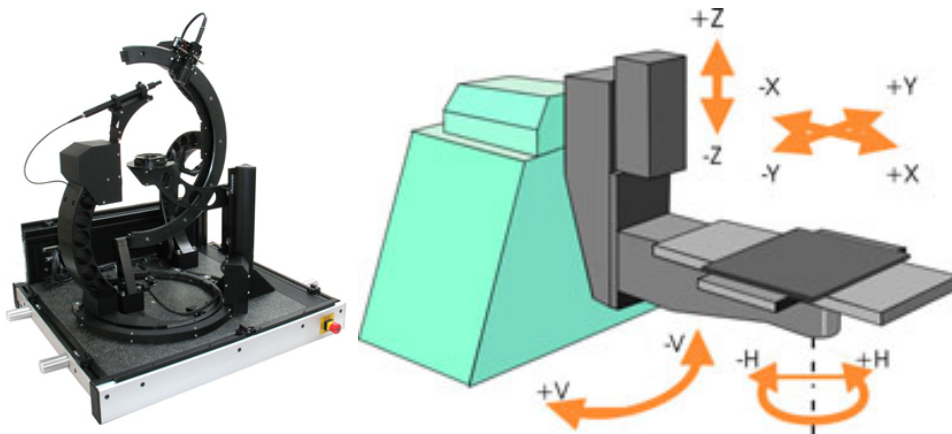


**Figure 3.2:** Goniophotometer.

Left: An example of a goniophotometer [24].

Right: A possible goniophotometer operation illustration [25].

The luminous intensity distribution of a light fixture is calculated measuring its illuminance at a given distance in all possible directions in space. Light sources are rarely spatially homogeneous, leading to the questions on which direction and how much solid angle should be used to carry out the measurement. A goniophotometer measures the spectral radiant flux distribution of a light source from many different angles around the source, and the results can be integrated to form a combined spectral radiant flux distribution for the light source.

A laboratory goniophotometer normally consists of a rotating light source holder, a fixed photometer, and, depending on the design, can have also a rotating mirror.

One possible measurement procedure consists on rotating the light source around the mirror at a fixed radius, whereby the mirror deflects the light emitted by the test object towards a photometer. Using a mirror, the test objects can be positioned in such a way that they remain in their designated position throughout the test procedure. This is essential when testing light sources whose photometric performance is orientationally sensitive [26].

Besides measuring luminous intensity, the goniophotometer can also measure illuminance. Integrating all the measurements along an imaginary sphere, the goniophotometer can also

calculate the total luminous flux emitted by a light source, this way emulating and replacing the high-cost integrating sphere.

### 3.3 Lux Meter

The lux meter is handy device to measure illuminances in a practical way. It also serves the purpose of calibration in this work, as the common photodiodes have a spectral sensitivity that goes off the visible range (they have the silicon responsivity, 190–1100 nm). As the luxmeter filters the non-visible range, it is a good way to calibrate the measurements in respect to a given light source (a string of LEDs for example).



**Figure 3.3:** ISO-TECH ILM350 used in the laboratory.

The measured illuminance is directly displayed in lux (lx). In general lux meters conform with international specifications [27, 28, 29], making them extremely reliable. The lux meter used in the work is the ISO-TECH ILM350 depicted in Fig. 3.3.

# Chapter 4

## LED Light Fixtures Analysis

The basic requirements of a light fixture are that it must comply with the following aspects [30]:

- Provide support and electrical connection to the lamp or lamps within it;
- Control and distribute the light from the lamp;
- Keep the operating temperature of the lamp within the prescribed limits;
- Be easy to install and maintain;
- Have a pleasing appearance;
- Be economically viable.

Light fixture definition present on the international standards [31]:

“Apparatus which distributes, filters or transforms the light transmitted from one or more lamps and which includes all the parts necessary for supporting, fixing and protecting the lamps, but not the lamps themselves, and where necessary circuit auxiliaries together with the means for connecting them to the supply.”<sup>1</sup>

Other common definitions about LED light fixtures:

- Light fixtures are complete lighting units that include a lamp or lamps, optics, ballasts or drivers, power supplies, and all other components necessary to have a functional lighting solution. For LEDs, light fixtures must also help to manage heat if the devices are to perform well [32].
- The combination of a module or a light engine with control gear to form a lighting system is described by the term LED light fixture. The fixture also defines the optical system in conjunction with the light source and functions simultaneously as a heat sink, if required [33].

---

<sup>1</sup>A luminaire with integral non-replaceable lamps is regarded as a luminaire except that the tests are not applied to the integral lamp or integral self ballasted lamp.

A LED lamp (or LED light bulb) is a solid-state lamp that uses LEDs as the source of light. LED lamps offer long service life and high energy efficiency, but initial costs are higher than those of fluorescent and incandescent lamps. Chemical decomposition of LED chips reduces luminous flux over life cycle as with conventional lamps.

General-purpose lighting needs white light. LEDs emit light in a very small band of wavelengths, emitting light of a color characteristic of the energy bandgap of the semiconductor material used to make the LED. To emit white light from LEDs, requires either mixing light from red, green, and blue LEDs, or using a phosphor to convert some of the light to other colors.

A single LED is a low-voltage solid-state device and cannot be directly operated on standard high-voltage AC power without circuitry to control the current flow through the lamp. In principle a series diode and resistor could be used to limit the current and to control its direction. This would be very inefficient since most of the applied power would be dissipated by the resistor, hence the necessity of a means to effectively convert AC power into DC to operate the LEDs correctly and efficiently.

One of the differences of LED light in respect to other light sources is the directional light. LEDs typically emit light in a more predominant direction as opposed to other artificial light sources. Thus illuminating a flat defined area by LED light, requires less luminous flux compared to light sources which would need reflectors or lenses to do the same.

For illuminating in  $4 \cdot \pi$  sr, the benefits of LED are smaller, but the geometry limitations can be compensated by the optical design. LED lamps are used for both general and special-purpose lighting.

## 4.1 LED Module

An LED can be considered to resemble a diode because it represents a chip of semiconducting material that is doped or impregnated with impurities to form a p-n junction. Similar to a diode, current easily flows from the p-side to the n-side of the semiconductor via a forward-bias potential, but not in the reverse direction.

When an electron crosses the barrier and meets a hole, it falls into a lower energy level and releases energy in the form of a photon (Fig. 4.1, left). The photon is a carrier of electromagnetic radiation of all wavelengths. The actual wavelength of light generated and its color that corresponds to the emitted wavelength is dependent on the band gap energy of the materials used to form the p-n junction (Fig. 4.1, right). For example, for silicon or germanium diodes, the electrons and holes combine via a forward-bias voltage such that a nonradiative transition occurs, which results in no optical emission as the semiconductors represent indirect band-gap material. However, through the initial use of gallium arsenide and other materials, a direct band gap with energies corresponding to near-infrared, visible, or near-ultraviolet light could be generated by the evolving LED.

LEDs used for lighting purposes are substantially different of the simple ones, because

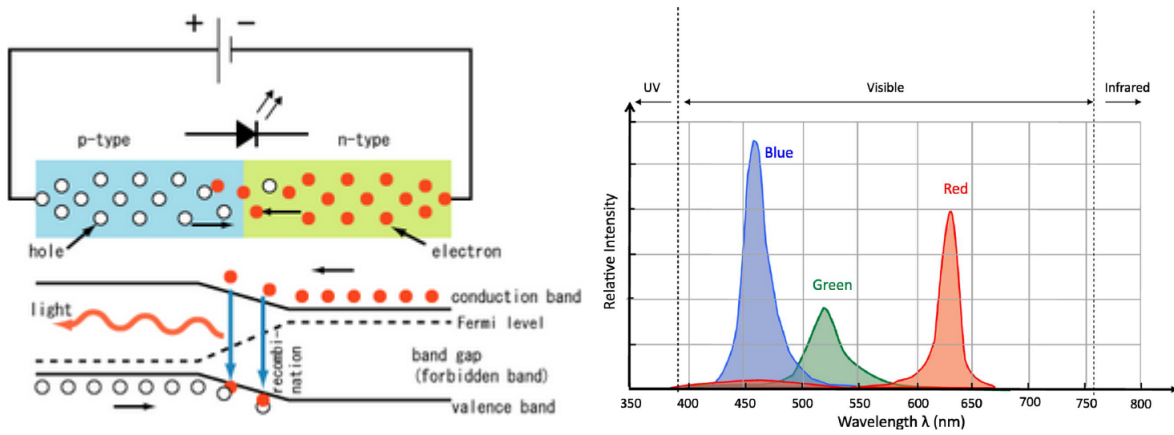


**Figure 4.1:** LED Light.

Left: LED color wavelength generation [34].

Right: Typical spectrum of “white” light created by mixing the output of red, green, and blue monochromatic LEDs [35]. Relative intensity is represented in arbitrary units.

of the high currents involved that can range from 350 mA to around 1 A or more. Taking that in account their construction is different and normally they are attached to a heatsink for heat dissipation and for mechanical and light fixture construction purposes. A diagram depicting the constitution of a typical lighting LED and a close-up of two LEDs present on a ARQUILED LED string used in the tests, are shown in Fig. ??.

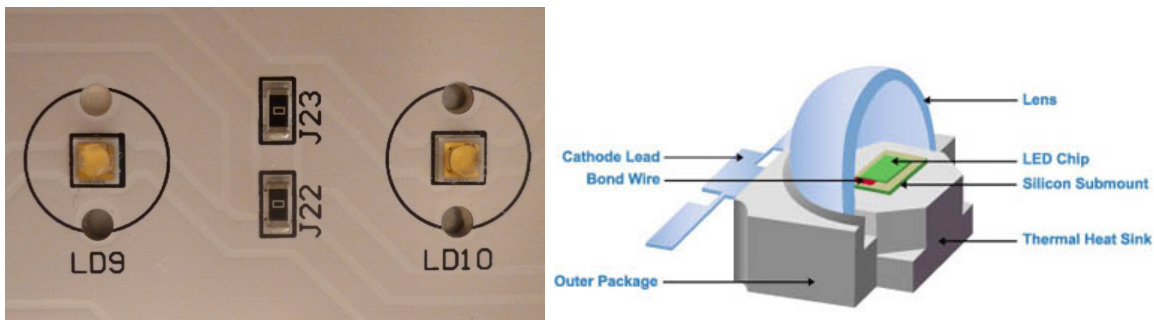


**Figure 4.2:** LED's in detail.

Left: Close up of the high power LED's present on the ARQUILED strings.

Right: Typical composition of a LED for lighting purposes [36].

### 4.1.1 White LED Energy Conversion

When radiant efficiency increases, luminous efficacy of a source also increases proportionally. The theoretical maximum for any light spectra is 683 lm/W which corresponds to the 555 nm monochromatic radiation. A fluorescent lamp can convert approximately 25% of the electrical energy into radiant energy in the visible spectrum [37].

For white light, an ideal 5800 K black-body, truncated to 400–700 nm (ideal "white" source), as shown on Fig. 4.3, has an efficiency of 251 lm/W. This corresponds to a radiant efficiency of 37% [38].

Designing a LED color consists basically in the choice of the semiconductor material. For



low-frequency (red, infrared) the material must have a low bandgap energy, while for a blue or UV LED must be a high-bandgap semiconductor. With this strategy various colors of the visible spectrum are possible to obtain, the problem is that they are monochromatic, and to design a white LED, it would be necessary to design a semiconductor with many bandgap energies at once.

There are two main process to overcome this difficulty, mixed-color white light and phosphor-converted white light.

One approach is to mix the light from several colored LEDs to create a spectral power distribution that appears white. By locating red, green and blue LEDs adjacent to one another, and properly mixing the amount of their output, the resulting light is white in appearance [39].

Another approach to generating white light is by use of phosphors together with a short-wavelength LED. For example, when one phosphor material used in LEDs is illuminated by blue light, it emits yellow light having a fairly broad spectral power distribution. By incorporating the phosphor in the body of a blue LED with a peak wavelength around 450 to 470 nanometers, some of the blue light will be converted to yellow light by the phosphor. The remaining blue light, when mixed with the yellow light, results in white light.

Both of these processes imply loss of radiant efficiency (only the 555nm green wavelegh is 100% efficient).

The main future developments at LED luminaire level are expected to be on external quantum efficiency of the LED device followed by improvements of fixture and optics efficiency. Producing white light using color-mixing gives the highest energy-efficiency potential at a system level in comparison to fixtures using phosphor-converted white LEDs [40].

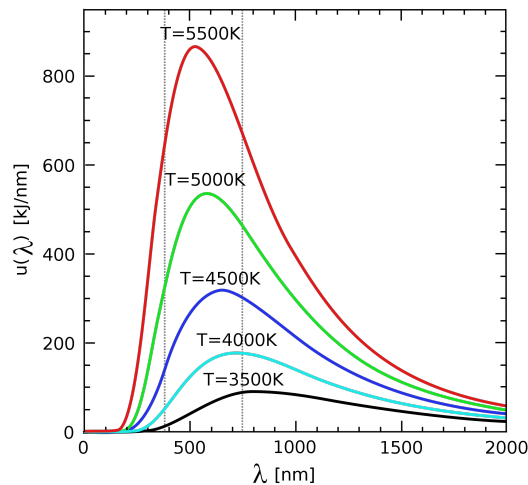


**Figure 4.3:** Spectral radiance of a black body. Energy outside the visible wavelength range ( $\sim 380\text{--}750$  nm, shown by grey dotted lines) reduces the luminous efficiency [41].



### 4.1.2 LED Thermal Runaway

LED temperatures of operation are intrinsically connected with electrical losses because the driver will try to compensate the additional need of current caused by the thermally induced decrease on  $V_f$ . As LEDs heat up, the forward voltage drops and the current passing through the LED increases. The increased current generates additional heating of the junction, and, although in this process the light output increases, the efficacy decreases [42]. If nothing limits the current, the p-n junction will fail due to the heat. This phenomenon is referred to as thermal runaway.

The light output variation and lifetime issues resulting from voltage variation and voltage changes can be eliminated by driving LED light sources with a regulated constant-current power supply. Therefore, constant current drivers are generally recommended for powering LED light sources in parallel with the use of heatsink or a good thermal design.

## 4.2 LED Driver

The most important element of the illumination system is the light source. It is the principal determinant of the visual quality, economy, efficiency, and energy conservation aspects of the illumination system. An electric light source is a device, which transforms electrical energy, or power (in watts), into visible electromagnetic radiation, or light (lumens). The rate of converting electrical energy into visible light is called luminous efficacy and is measured in lumens per watt.

A LED driver is an electrical device that regulates the power to an LED or string(s) of LEDs. What makes a driver different from conventional power supplies is that an LED driver responds to the ever-changing needs of the LED, or circuit of LEDs, by supplying a constant amount of power to the LED as its electrical properties change with temperature.

- The main function of a driver is to limit the current regardless of input and output conditions across a range of operating conditions. In other words it must behave as an ideal current source;
- AC-DC power conversion and driver regulation can be merged together into a single driver or separated into two stages;
- The arrangement of LEDs and the light fixture specifications dictate the fundamental driver requirements;
- Isolated solutions means there is no physical electrical connection between the AC line voltage and the LEDs.

Given that the light output from a LED is proportional to the forward current drive, the “ideal” LED driver consists of a constant current source. The forward voltage of the LED can also vary, therefore, the amount of power delivered to the LED will fluctuate. Furthermore,

the brightness of LEDs also varies, as a function of the manufacturing process, which means that it is necessary to account for variations in both driver current and the forward voltage characteristics of the device.

Two primary topologies are used in order to properly bias the LED, as shown in Fig. 4.4. One topology is the traditional Buck regulator. The Buck topology is the most common DC-DC implementation since it is in many ways an “ideal source” providing a constant current output and very high output impedance.

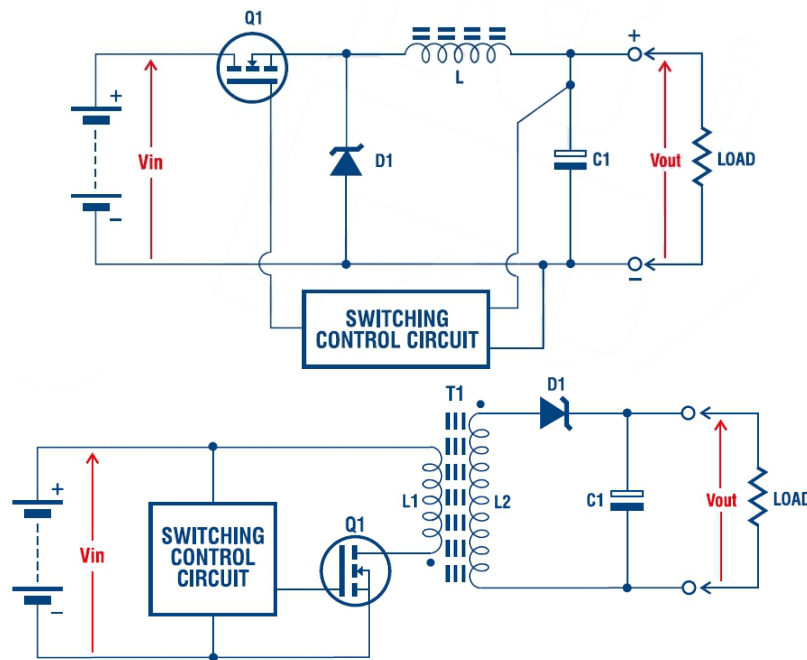


**Figure 4.4:** Common LED driver topologies [43].

Top: Buck converter (non-isolated).

Bottom: Flyback converter.

Another popular topology is the flyback regulator, and it is a compact, low cost, high efficiency (85%), isolated AC-DC converter solution for direct LED drive (Constant power is not important; it is controlling the current).

For a fluorescent lamp, the device equivalent to the LED driver is called a “ballast”. Ballasts also exhibit power loss that reduces the luminous efficacy.

### 4.2.1 Losses in LED Driver

Losses in a LED driver occur due to several factors, some related with the frequency of operation and others due to the duty cycle:

- Driving and switching losses to the MOSFETS/IGBTs. Increases with frequency, independent of duty cycle;
- Diode losses. Independent of frequency, Increases with duty cycle;
- Capacitor ESR losses. Decreases with frequency;

- Inductor resistance. Independent of frequency, increases with duty cycle.

#### 4.2.1.1 MOSFETs

Power loss in a MOSFET comes from two sources. Every MOSFET has a resistive element, so it dissipates power as current is conducted through the device. The resistive parameter is described as on-resistance, or  $R_{DS(ON)}$ . These conduction losses are inversely proportional to the size of the MOSFET; the larger the switching transistor, the lower its  $R_{DS(ON)}$  and, therefore, its conduction loss.

The other source of power loss is through switching losses. As the MOSFET switches on and off, its intrinsic parasitic capacitance stores and then dissipates energy during each switching transition (Fig. 4.5, left). The losses are proportional to the switching frequency and the values of the parasitic capacitances. As the physical size of the MOSFET increases, its capacitance also increases; so, increasing MOSFET size also increases switching loss.

MOSFETs with the lowest  $R_{DS(ON)}$  specification are the best to minimize losses. Also good heat dissipation is critical.

#### 4.2.1.2 Diodes

Diodes suffer from three sources of losses [44], depicted on Fig. 4.5 (right).

- Conduction losses, due to the forward voltage drop of the diode;
- Switching losses, due to the fact that a diode does not switch from conducting state to a non conducting state in zero time;
- Power diodes (Rectifiers) also conduct current when reversed biased. This reverse leakage is very temperature dependent. The conduction losses are proportional to current and the forward voltage drop of the diode.

The reverse leakage losses tend to be small, but in high voltage application, the leakage current times the applied voltage product may become appreciable.

Diodes with “Ultra Fast” specification and low forward voltage drop are the best to reduce losses.

#### 4.2.1.3 Capacitors

The dominant loss for capacitors used in the LED driver (and in general SMPS applications) is due to the ESR (Effective Series Resistance). The ESR is due to the physical construction of a capacitor including the resistance of the internal interconnect, and the behavior of the electrolyte or other material used as the insulator between the capacitor plates.

These internal processes that impede the flow of current into and out of the capacitor are modeled as a resistor in series with an ideal capacitor.

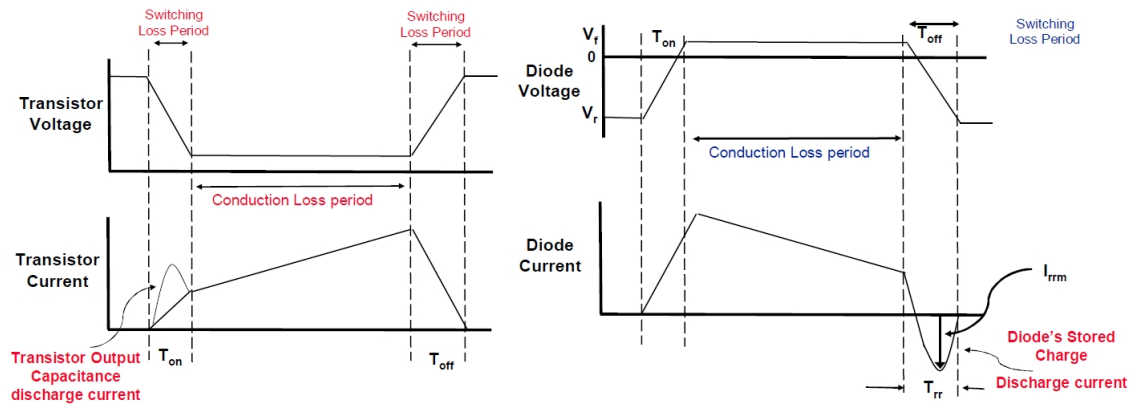


**Figure 4.5:** MOSFET and diode waveforms [44].

Left: MOSFET losses.

Right: Diode losses.

Possible solutions to minimize capacitor losses consist in the use of capacitors with low ESR and derating, voltage derating, and good heat dissipation [45].

#### 4.2.1.4 Magnetic Losses

The losses in magnetic components are primarily due to three issues: hysteresis losses, eddy current losses, and losses in the windings that surround the magnetic core.

The hysteresis loss is due to the resistance of the flipping of the magnetic domains in the material. The magnetic core is structurally similar to a shorted conductor loop passing through the magnetic field. The induced current in the core will dissipate energy.

To reduce eddy current losses, core materials have been developed that suspend magnetic particle in a binder with higher resistivity such as epoxy.

The windings used in magnetic components for SMPS applications experience losses due to winding resistance ( $I^2 \cdot R$  losses), and the skin effect [46].

## 4.3 Fixture

Manufacturers of LED lights provide light flux as the sum of the fluxes of all the LEDs. This value is given by characteristics of the LEDs at given current, multiplied by the number of LEDs, which are built in a lamp.

Real flux lamp is lower than this value, it is necessary to take into account losses in the optics used by the lamp and the losses of the glass that covers and protects LED diodes. The real delivered luminous flux and luminous flux of LEDs are the same only when the lamp does not use optics and LEDs are not covered with protective glass or any other protection and the fixture itself does not affect the lumen output in any way.

So two types of light losses within the fixture itself can be considered:

- Optical and geometry derived losses;
- Losses within the light fixture itself.







**Figure 4.6:** Some types of LED optical designs.

Left: LED bulb.

Center: LED light fixture for use in public lighting.

Right: LED lamp with minimal lumen output loss due to its conical form.

Light Source	Light Source Efficacy	Coefficient of Utilization	Fixture Efficacy
CFL	 65lm/W	 54%	35 lm/W
XLamp XR-E Neutral White	 58 lm/W	 77%	44 lm/W

**Figure 4.7:** Losses within the fixture in two different cases [47].

### 4.3.1 Optics

Because of the narrower light emission of LEDs in comparison with other light sources, the optics play an important role in the light distribution. Depending on the LED light fixture application, the optics can have different forms to properly distribute the luminous flux on the evolving space. This geometry designs are normally made at the cost of some luminous power. Several forms of LED optical designs are projected for various lighting applications, some of them shown on Fig. 4.6.

### 4.3.2 Fixture Housing Light Loss

Fixture light loss occurs when light rays from the light source strike the fixture housing before hitting the target. Some light is absorbed by the fixture housing, while some is reflected back into the fixture. The efficiency of the fixture is dictated by placement of the light source, the shape of the fixture housing, and materials used in the fixture housing.

As Fig 4.7 shows, the directional nature of LED light enables much higher fixture efficiencies than those possible with omni-directional light sources.

## 4.4 Other Efficiency Losses

There are other efficiency loss factors that will not be covered on this work but are an ongoing issue of research. They are called scotopic superiority, lumen maintenance and CRI.

Scotopic superiority consists in engineering the LED spectrum carefully so that it takes advantage of the scotopic vision. This way it is possible to obtain a better efficacy especially at night in open spaces (roads, parks, etc.) [48].

Lumen maintenance deals with long term LED affecting issues, some easily recoverable (dirt affecting the optical part or evolving space reflections), and others non-recoverable (degradation of components and LED p-n junction). Methods to extract these degradation issues are covered in the international standards [49].

The color rendering index affects the efficiency, because in the process of creating a given color, for example white, there is luminous efficacy of radiation losses (ratio of luminous flux to radiant flux), and higher CRI normally implies less efficiency [50].

# Chapter 5

## Motivation and Development of Goniophotometer

The integrating sphere is expensive and is beyond the scope of this project, so another alternative was chosen.

The goniophotometer emulates the integrating sphere, measuring several points of luminous intensity scattered spacially and then performing interpolation on them to obtain a spherical surface, like the one in the integrating sphere. Although this is a more cost effective solution, by no means is inferior, because it gives information about the spatial distribution of a radiation source and also the photometric properties of the light visible to the human eye in relation to a defined angular position.

In this work, for simplicity, a simple version of the goniophotometer will be projected. With only one degree of freedom, the apparatus will achieve the goal, rotating a circular arc around the fixed axis coincident with the luminous source.

### 5.1 Mathematical Background

The portion of the luminous intensity of a light source  $I(\omega)$  is better defined by subdividing the total solid angle ( $\Omega = \int d\omega = 4\pi$ ) into fractional solid angles, which can only be made by using a goniophotometer. Thus, the total luminous flux,  $\Phi_V$ , is calculated from  $\Phi_V = \int I(\omega)$ .

Let  $\theta$  and  $\varphi$  be the polar and azimuthal angles in a spherical coordinate system the origin of which is at the lamp location. The solid angle is equal to the area of the zone  $A$ , divided by the square of the radius  $r$ . Thus, for an elementary zone at an angle of  $\theta$  subtending an angle of  $d\theta$  the solid angle is

$$d\omega = \frac{dA}{r^2} = \frac{2 \cdot \pi \cdot r \cdot \sin(\theta) r d\theta}{r^2} = 2 \cdot \pi \cdot \sin(\theta) d\theta \quad (5.1)$$

For the zone extending from  $\theta_l$  to  $\theta_h$

$$\omega = 2 \cdot \pi \int_{\theta_l}^{\theta_h} \sin(\theta) d\theta = 2 \cdot \pi (\cos(\theta_l) - \cos(\theta_h)) \quad (5.2)$$

This value is called the zone factor and for convenience it is usual to divide the sphere into zones subtending equal angles of elevation  $\theta$  at the centre of the sphere. The spherical surface is divided into  $n$  meridians and  $m$  parallels and the luminous intensities  $I_{m,n}(\theta, \varphi)$  are measured at the cross points between parallels and meridians. To find the luminous flux in a zone the zone factor is multiplied by the average  $I_{m,n}(\theta, \varphi)$  in the directions of the zone. Thus, the total luminous flux emitted by the light source is calculated by

$$\Phi_V = \int_{\theta=0}^{\pi} \int_{\varphi=0}^{2\pi} I_{m,n}(\theta, \varphi) \sin(\varphi) d\varphi d\theta \quad (5.3)$$

The derivation of the total luminous flux from illuminance  $E(\theta, \varphi)$  is well suited to the realization of the standards of the luminous flux. In this approach the total luminous flux is calculated by  $\Phi_V = \int E(A) dA$ , where  $dA$  is the element of area that is illuminated by the light source at a photometric distance of  $r$ . So  $dA = d\omega \cdot r^2 = 2 \cdot \pi \cdot r^2 \cdot \sin(\theta) d\theta d\varphi$ . The same zonal factor method is used for finding the total luminous flux emitted by the light source here. Many national standard laboratories use this technique, where the total luminous flux is calculated by

$$\Phi_V = r^2 \int_{\theta=0}^{\pi} \int_{\varphi=0}^{2\pi} E_{m,n}(\theta, \varphi) \sin(\varphi) d\varphi d\theta \quad (5.4)$$

In practice, the integral is replaced by the following sum, considering

$$\Phi_V = 2\pi r^2 \sum_{\theta=0}^{\pi} \left[ \sum_{\varphi=0}^{2\pi} E_{m,n}(\theta, \varphi) [\cos(\theta_l) - \cos(\theta_h)] \right] \quad (5.5)$$

This equation will be used to calculate the total luminous flux emitted by the light source in the center of the goniophotometer. The acquired points of intensity will be multiplied by an adjacent area element. The sum of all areas will give the total luminous flux.

## 5.2 Construction Guidelines

The principle of operation of the device is a semicircular arc, with photodiodes inserted on it, that will rotate around a light source. The axis of rotation is fixed, as it is the light source, and, along the rotation the photodiodes will acquire measurements in defined intervals.

A crucial point is the integration of a rotary positioner that will rotate the circular arc. A diagram illustrating the mathematical modelling is shown in Fig. 5.1.

- The LED string or light fixture will be positioned on the center of the sphere, to obtain symmetry;
- The light source will be placed in the testing place with the help of a wooden support.



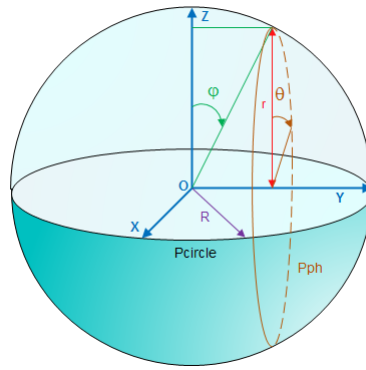


**Figure 5.1:** Scanning sphere referencial.



**Figure 5.2:** Goniophotometer built for the project.

- The rotation will be made on half hemisphere only, so half of a sphere will be scanned;
- On the circular arc, the angular displacement between the slots in which the photodiodes will be placed is regular and known (9 degrees);
- The scanned surface will be divided in slices, from which, a step angular displacement will be calculated. The arc will rotate in those defined regular intervals.
- With these guidelines the goniophotometer was built, and the resulting prototype shown on Fig. 5.2.

## 5.3 Goniophotometer Control and Data Acquisition

To control the goniophotometer and acquiring data from the photodiodes, the following hardware were used, connected as represented in Fig. 5.3.

### 5.3.1 National Instruments 6009

National Instruments 6009 is a data acquisition external device, easy to use and with plug and play USB connectivity. The device acquires voltage signals between -10 and +10

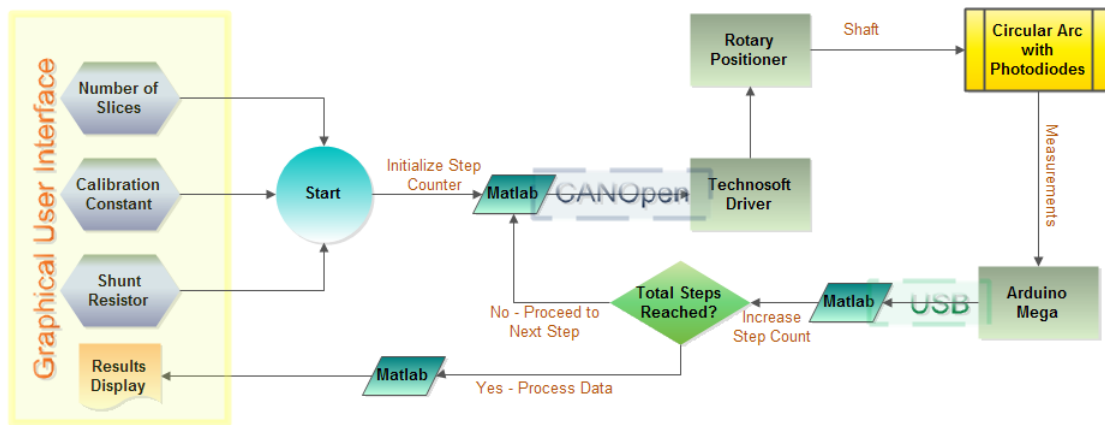


Figure 5.3: Goniophotometer control diagram.

volts, so, as the reverse light current is the quantity to be measured, and is typically of small value, a precision resistor of adequate value is used in the photodiode circuit to acquire voltage measurements.

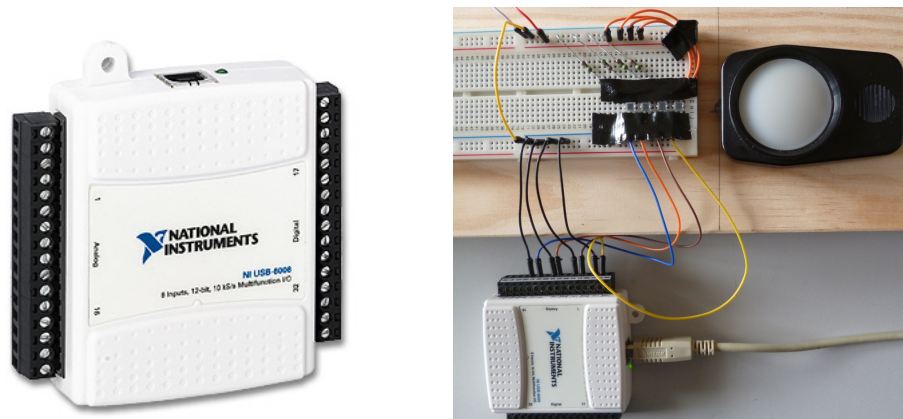


Figure 5.4: Photodiode measurements.  
Left: Acquisition board NI-6009 used as ADC.  
Right: NI-6009 used in photodiode calibration.

This acquisition board was used in all the stages of the work, but eventually it was found a limitation<sup>1</sup> on its use on MATLAB environment that prevented its use with more than 4 photodiodes, so an Arduino Mega was used, shown in Fig. 5.5. However, the NI-6009 was of great help on the testing and calibration. In Fig. 5.4 is shown the NI board and a detail of the calibration setup.

### 5.3.2 Arduino Mega

Initially a maximum of 8 photodiodes was planned to be inserted on the rim, corresponding to the number of input channels in (single ended mode) of the NI-6009 Data

<sup>1</sup>This limitation involves using more than four channels in single ended mode in the MATLAB Data Acquisition Toolbox, for which a solution was not encountered, at least in a practical way, at the time of this work.

Characteristic	Description
Microcontroller	ATmega1280
Operating Voltage	5V
Input Voltage (Recommended)	7-12V
Input Voltage (Limits)	6-20V
Digital I/O Limits	54 (of which 15 provide PWM output)
Analog Input Pins	16 (10-bit resolution)
DC Current per I/O Pin	40 mA
DC Current for 3.3V Pin	50 mA
Flash Memory	128 KB of which 4 KB used by bootloader
SRAM	8 KB
EEPROM	4 KB
Clock Speed	16 MHz

**Table 5.1:** Arduino ATmega1280 characteristics.

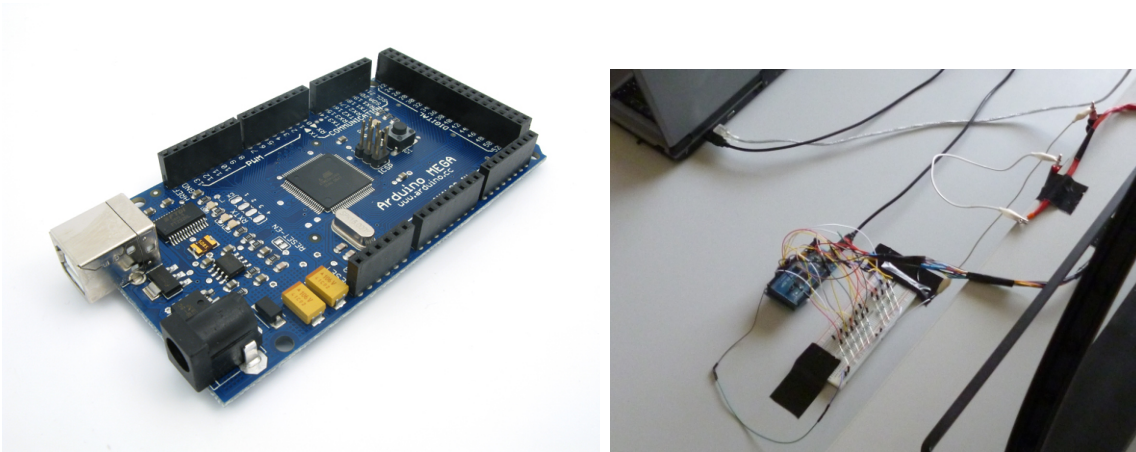


**Figure 5.5:** Arduino Mega.

Left: Arduino Mega microcontroller board.

Right: Setup to acquire the photodiode measurements.

Aquisition Device. But later, was decided to use an Arduino Mega, and so 10 photodiodes were used.

The Arduino ATmega1280 has less resolution than the NI USB-6009 acquisition board, however that loss is not important and it is largely compensated for the possibility of the use of a greater number of photodiodes.

The Mega has 16 analog inputs, each of which provides 10 bits of resolution (i.e. 1024 different values). By default they measure from ground to 5 volts. On Table 5.1, are presented the main operational characteristics of Arduino Mega.

### 5.3.3 Rotary Positioner Micro-Controle

The device that will rotate the circular arc around the luminous source is a rotary positioner constituted by a UR80 stage and a UE-31-PP motor from Micro-Controle<sup>2</sup>. The

<sup>2</sup>Now part of Newport Corporation.

Characteristics	Value
Drive	motorized (stepping) - UE-31-PP
Bearings	single row ball
Travel Range ( $^{\circ}$ )	unlimited
Accuracy on Axis ( $10^{-3}^{\circ}$ )	20
Reapeatability ( $10^{-3}^{\circ}$ )	2
Hysteresis ( $10^{-3}^{\circ}$ )	6
Resolution ( $10^{-3}^{\circ}$ )	1
Wobble ( $10^{-6}$ rad)	50
Centered Load Capacity (N)	200
Mass (Kg)	1 to 2

**Table 5.2:** UR 80 Stage characteristics

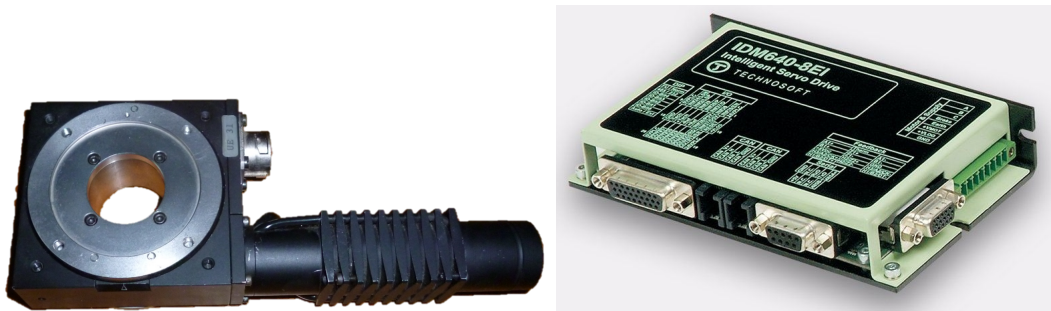


**Figure 5.6:** Rotary positioner control.  
 Left: UR80 stage and UE-31-PP motor ftom Micro-Controle.  
 Right: Technosoft IDM640-8EI Driver.

characteristics of the positioner are indicated in the Table 5.2.

This rotary positioner is operated through a Technosoft IDM640-8EI driver (Fig. 5.6). This driver communicates with MATLAB through the CANopen<sup>3</sup> communication protocol.

---

<sup>3</sup>CANopen is a standardized application for distributed automation systems based on CAN (Controller Area Network).

# Chapter 6

## Error Sources and Calibration

Although the measurements will follow the standards and try to achieve the maximum precision and accuracy, the scope of this work limits that objective, and some commitments have to be made in order to carry on with the tests:

- Since lux is a measure for visible light only, near-infrared radiation (800 nm to 1100 nm) where silicon detectors have their peak sensitivity is not taken into account. Unfortunately, the near-infrared emission of various types of light sources varies widely. As a result, light current measurements carried out with different light sources (but the same lux and color temperature calibration) may result in readings that differ up to 20 % [51]. The simplest way to overcome this problem is to calibrate some photodetectors against a reference light source or a luxmeter to find a relation;
- The detectors used are the general purpose BPW34 photodiodes<sup>1</sup>, with angular displacement and relative spectral response depicted on Fig. 6.1 (right). These photodiodes have a high sensitivity outside the visible spectrum, so a large discrepancy between the illuminance relation given by the datasheet and the lux meter is expected. This will especially be true with the white LED light, because of the high blue wavelength component;
- The photometry tests will be made at night, trying to recreate a dark room. But there is always some stray light that may influence the tests;
- The photodiodes will be used in photoconductive mode, and some noise in the measurements will occur (due to the Johnson-Nyquist effect [53] in shunt resistors), that will have to be taken into account in the calibration process;
- The angular displacement has an influence on measurements. A method for fixing the photodiodes will have to be found, in order to minimize that effect;

---

<sup>1</sup>Although the BPW34 are general purpose photodiodes, in practice, to obtain accuracy in the measurements, the calibration process is always necessary.



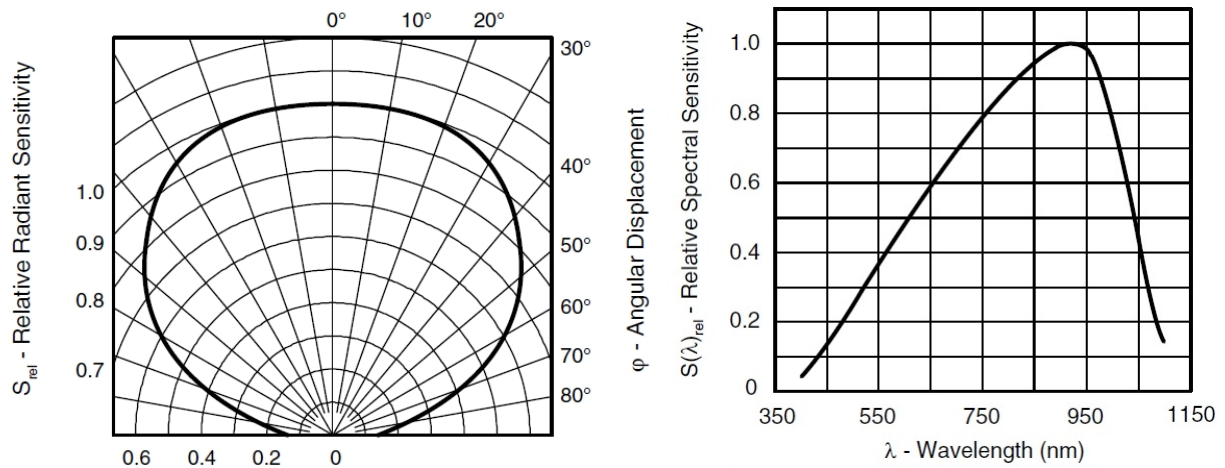


**Figure 6.1:** BPW34 Photodiode [52].

Left: Angular displacement.

Right: Spectral response.

- A mechanical stabilization of the light fixture will have to be arranged. The support for the luminary is not ideal, although it was well measured;
- In the process of cutting the rim arc for insertion in the goniphotometer axis there was some deformation caused to the arc, although a support was fixed to attenuate that effect. This caused some minor eccentricity on the circular scanning arc;
- The rotation axis has a slight eccentricity as well.

## 6.1 Calibration

To assure the accuracy of the measurements made with the photodiodes, there is the need of calibration.

Depending on the visible color of the LEDs, manufacturers and methods of construction, there are different spectrum emissions [54]. The photodiodes, depending on their type and fabrication process also have a variable spectral sensitivity, different from the visible spectral range.

In order to find a relation between the spectral emission of the artificial light sources and sensitivity of the photodiodes, the light measurements must be made against a lux meter, so the fraction relation of the visible range detected by the photodiodes can be extracted.

Other motive for calibration is to account the effect of the noise in the measurements due to the effect of the shunt resistors, the ADC itself, cables and terminal contacts.

On Fig. 6.2 there is a spectral emission of a cool white LED (5000K-6000K), similar to those that will be tested. As it can be seen, this spectral range differs much from the sensitivity of the photodiodes used in the work (Fig. 6.1, right).

It is expected that the light emitted by the LEDs, (especially the cool white LEDs present in the strings that will be used) will have a small impact on the sensitivity of the BPW34 photodiodes, that will reflect on the reverse current value.

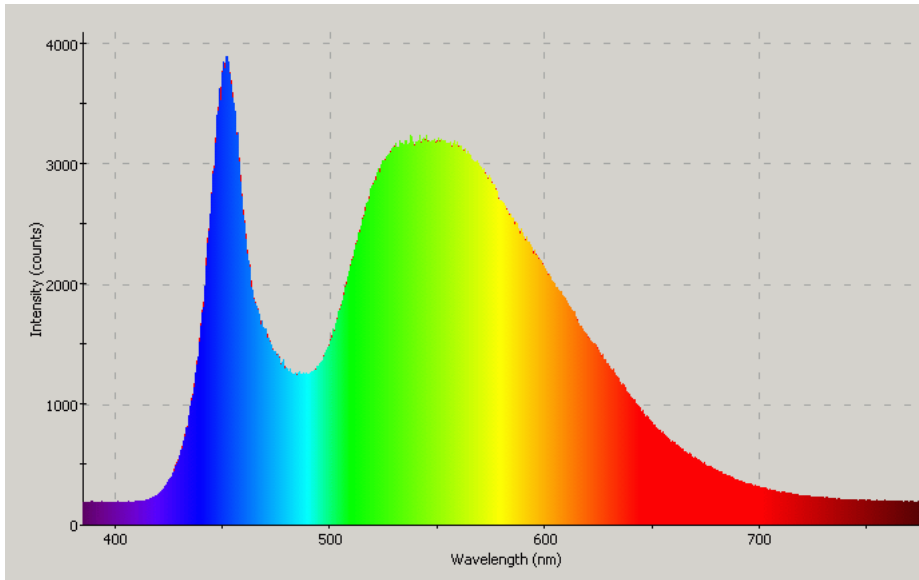


**Figure 6.2:** Spectral response of cool white LEDs [55].

## 6.2 Photodiode

The photodiode is a special kind of diode that reacts to the light spectrum received, outputting a related current. This current for the most part varies linearly with the luminous flux received, except in very high luminosity where saturation occurs.

In Fig. 6.3 (right) that relation can be seen, in photodiode mode (3<sup>rd</sup> quadrant).

### 6.2.1 Reverse Current

The reverse-bias operation allows the photodiode to be used as a light intensity-to-voltage transducer. The current that flows by the anode maintains a linear relation with the illuminance, which is normally supplied by the manufacturer on the photodiode datasheet.

To measure that reverse current,  $I_{REV}$ , a shunt resistor,  $R_{SHUNT}$  is placed in the circuit. That way the measurements can be made by a ADC in voltage,  $V_{ADC}$ .

So the following relations are present:

$$V_{ADC} = R_{SHUNT} \cdot I_{REV} \quad (6.1)$$

$$E_V = I_{REV} \cdot K_{PH} \quad (6.2)$$

Joining the equations 6.2.1 and 6.2.1, the illuminance value is given:

$$E_V = K_{PH} \cdot \frac{V_{ADC}}{R_{SHUNT}} \quad (6.3)$$

The shunt resistor has to be chosen in a way that doesn't let the input voltage exceed the Arduino ADC limit 5V.

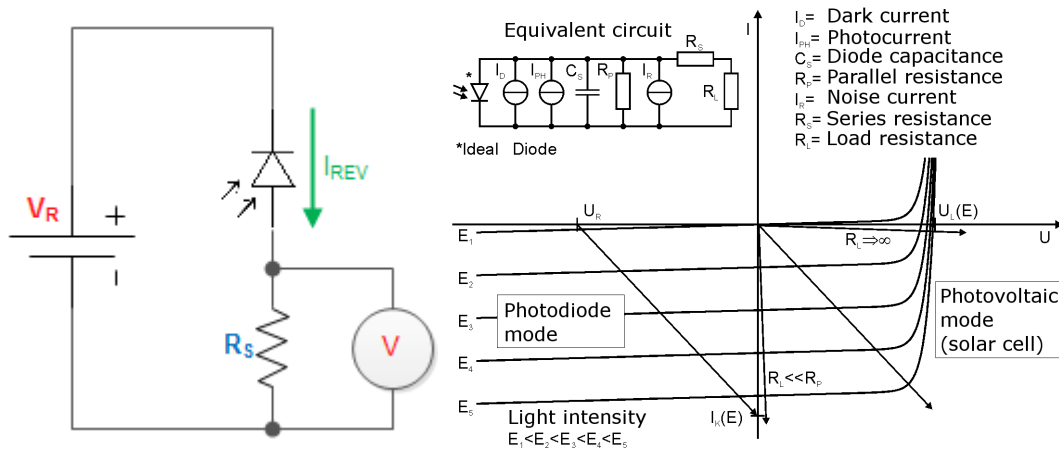


**Figure 6.3:** Photodiode measurements.

Left: Measurement circuit for photodiode mode.

Right: I-V curve of a photodiode and the equivalent circuit [56]. The linear load lines represent the response of the external circuit. The points of intersection with the curves represent the actual current and voltage for a given bias, resistance and illumination.

Distance [cm]	100	90	80	70	60	50	45	40	35	30
ILM [lx]	348	427	527	676	910	1320	1710	2120	2980	3800
Ph's [lx]	57,8	91,2	108,2	134,9	154,3	240,4	284,2	364,7	508,7	637,1

**Table 6.1:** Calibration measures using a LED string with 9 LEDs.

## 6.3 Calibration Results

To calibrate the photodiodes to the LED strings present in the laboratory, measurements were made at various distances to confirm the linearity relation between the two types of detectors and also to extract a calibration relation.

On Table 6.1 are presented the calibration data of the photodiodes. After fitting the values to a linear function  $f(x) = C_{PH} \cdot x$ , a value of  $C_{PH} = 5,862$  is found, expressing the calibration constant relation for this light source.

The lamps tested were also calibrated, making measurements at a given distance (Table 6.2). That distance was chosen in a way that it would not be too close to the detectors (to avoid higher discrepancies related to the angular displacement), but also would not be too far (the illuminance levels would be lower thus more susceptible of noise).

As expected, the photodiodes weight the LED light with a low value due to its low sensitivity in the blue wavelength. In the contrary the light of the incandescent lamps (including the halogen one) is well weighted due to the high sensitivity BPW34 has in the infrared zone,

	LED LAMP	CFL	HAL	ILB	LED STRING
Light Meter	770	1850	250	3020	1320
Photodiodes	141	490	206	2513	240,4
Calibration Constant	5,461	3,776	1,214	1,202	5,862

**Table 6.2:** Calibration constants for the various light sources.



where incandescent lamps have a high spectrum magnitude [57].

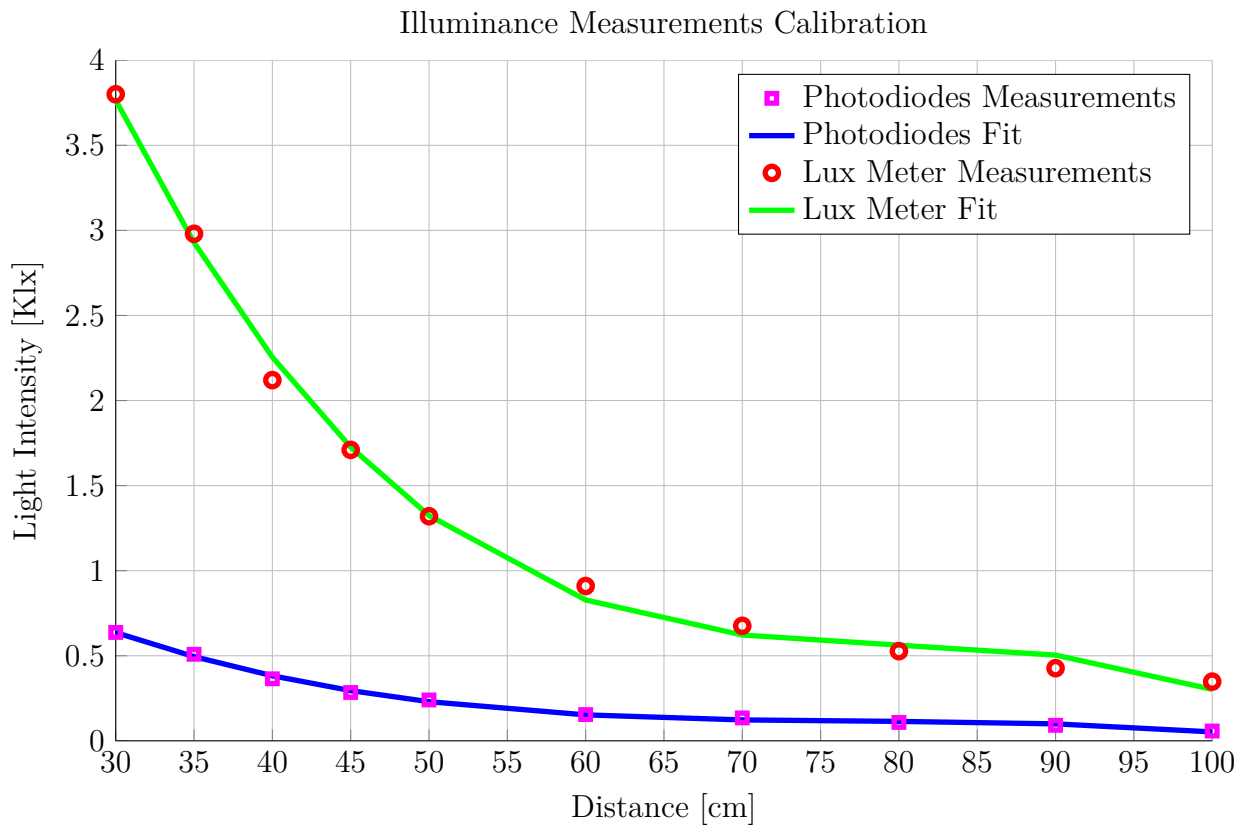


**Figure 6.4:** Illuminance relation with the distance to luminous source (the LED string).

# Chapter 7

## Experimental Results

The first tests will be made on commercial lamps of various types, so a comparison can be made in terms of their electrical and photometric characteristics.

A special care will be taken on the LED lamp analysis, and after the photometric testing it will be teared down apart so his internal constitution can be studied, in particular the driver. After that, the LED driver of the aquired lamp will be compared to some other drivers present on the lab, from various manufacturers with different cost and characteristics.

The driver of the aquired lamp will have his own load, the LEDs that came with it. For the remaining drivers LED strings will be used, in parallel or in series according to the driver's output voltage and current specifications. Each LED present on those strings draws 350 mA in nominal operation, but can be safely overdriven to higher values for a short time.

### 7.1 Commercial Lamps Testing

The commercial lamps tested were choosen taking in account the different technologies of each one, in order to take some conclusions about their luminous efficacy. They have also diferent shapes and formats, and that will have an impact in the light fixture efficiency itself, because some luminous flux will be lost due to internal reflections and lamp absorptions.

A brief description of the different lamp technologies tested is given below:

- Compact Fluorescent Lamp (CFL) is a fluorescent lamp designed to replace an incandescent lamp. This lamp is a gas-discharge lamp that uses electricity to excite mercury vapor. The excited mercury atoms produce short-wave ultraviolet light that then causes a phosphor to fluoresce, producing visible light. A fluorescent lamp converts electrical power into useful light much more efficiently than incandescent lamps, and most types of CFL lamps fit into light fixtures formerly used for incandescent lamps;
- Incandescent Light Bulb (ILB) is an electric light which produces light with a filament wire heated to a high temperature by an electric current passing through it, until it glows. This type of technology is being phased out due to his low energy efficiency;

ID	Brand	$P$ [W]	PF	$\Phi_V$ [lm]	CRI	CT [K]	Cost [€]
CFL	LEXMAN	18	0,6	1140	80	4000	12
HAL	PHILIPS	50	1	550	100	2800	2
ILB	PHILIPS	40	1	415	100	3000	1
LED	OEM	6	0,7	415	80	5000	25

**Table 7.1:** Various types of lamps to be tested.

- A halogen lamp, is an incandescent lamp that has a small amount of a halogen such as iodine or bromine added. A Halogen lamp can be operated at a higher temperature than a standard gas-filled lamp of similar power and operating life, producing light of a higher luminous efficacy and color temperature;
- LED light bulb, is designed to replace lower efficiency incandescent lamps or other lamp types (halogen spot, CFL or sodium-vapor lamp), reusing his socket (E27 or other). It's bulb shape is a challenging design for LED lighting, due to the necessity to perform similarly, in terms of light distribution, to the incandescent bulbs.

In Table 7.1 are summarized the characteristics of the lamps used in the tests.

The total luminous flux given by the manufacturers is assumed correct, since is mandatory that the lamps are tested by certified laboratories before being commercialized.

### 7.1.1 Light Fixture

Taking in account the characteristics of the goniophotometer built, a light fixture was chosen to insert the lamps. It was a technical one, with a parabolic shape common to various types of light fixture applications (office desks, gardens, public areas, etc.). The fixture has a metallic reflecting surface designed to reflect most of the light outwards (Fig. 7.1).



**Figure 7.1:** Light fixture used to accomodate the lamps.

The lamps selected for testing were choosen also for their height, since they must completely fit in the volume defined by the fixture dimensions. This is necessary so the luminous flux do not escape below the scanned hemisphere.

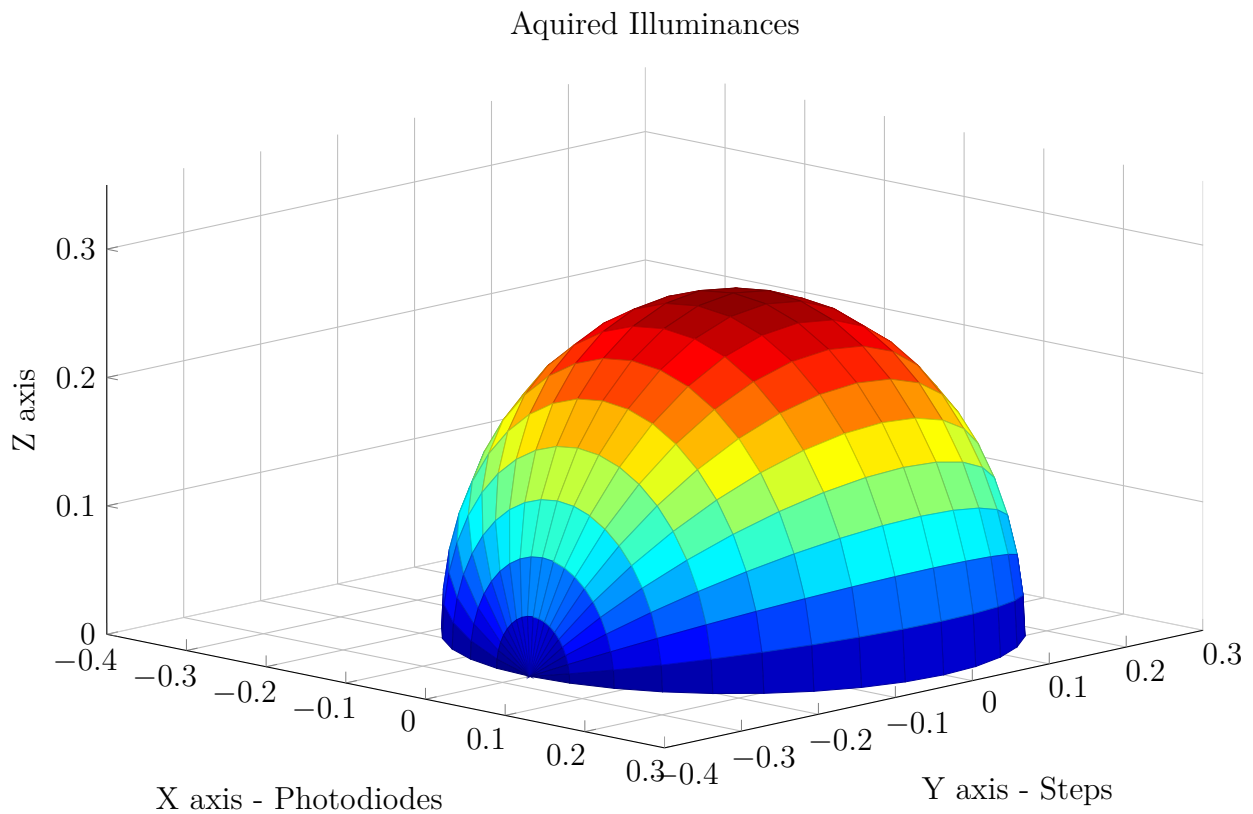


**Figure 7.2:** Sphere discretization obtained with 20 slices and a fixed displacement of 9 degrees between the photodiodes.

The application of the algorithm to calculate the total luminous flux, with a discretization of 20 slices of hemisphere, resulted in the discretized sphere seen in Fig. 7.2. The illuminances measured with the photodiodes translated in areas, with the higher values of illuminance at the region above the center of the sphere and the lower ones in the periphery.

### 7.1.2 Results of Lamp Testing

The light fixture was inserted in a wooden support designed so the luminary surface is coincidente with the axis of rotation, as shown in Fig. 7.3. The tests were made at night, an some time was given after the lamps were turned on, in order they stabilize and deliver a constant luminous flux.

The results obtained were summarized in the Table 7.2. “LED1” refers to the LED bulb in its original form, with the optical part, and “LED2” refers to the LED bulb without the optical part, with the SMD LEDs exposed.

This way, the effect on the luminous efficacy of the optical part of the LED lamp can be evaluated.

The chart in Fig. 7.4 shows a comparison between the rated luminous efficacy,  $\rho_{VN}$ , and the measured with the fixture,  $\rho_{VFIX}$ . The absolute efficacy difference,  $\rho_{VN} - \rho_{VFIX}$ , gives an indication of the magnitude of luminous loss in the fixture, and the efficiency in delivering the luminous flux by the fixture is expressed by  $\eta_{FIX}$ .



**Figure 7.3:** Lamp Testing.  
 Left: Compact Fluorescent Lamp (CFL).  
 Right: LED Lamp.

ID	$P_N$ [W]	$\Phi_{VN}$ [lm]	$\rho_{VN}$ [lm/W]	$\Phi_{VFIX}$ [lm]	$\rho_{VFIX}$ [lm/W]	$\rho_{VN-VFIX}$	$\eta_{FIX}$ [%]
CFL	18,27	1140	62,4	849,3	46,49	15,91	74,5
HAL	48,52	530	10,92	507,5	10,46	0,46	95,8
ILB	39,64	415	10,47	378,2	9,54	0,93	91,1
LED1	5,93	420	70,83	367,5	61,97	8,86	87,5
LED2	5,93	446,9	75,36	446,9	75,36	0	100

**Table 7.2:** Results of lamp testing.

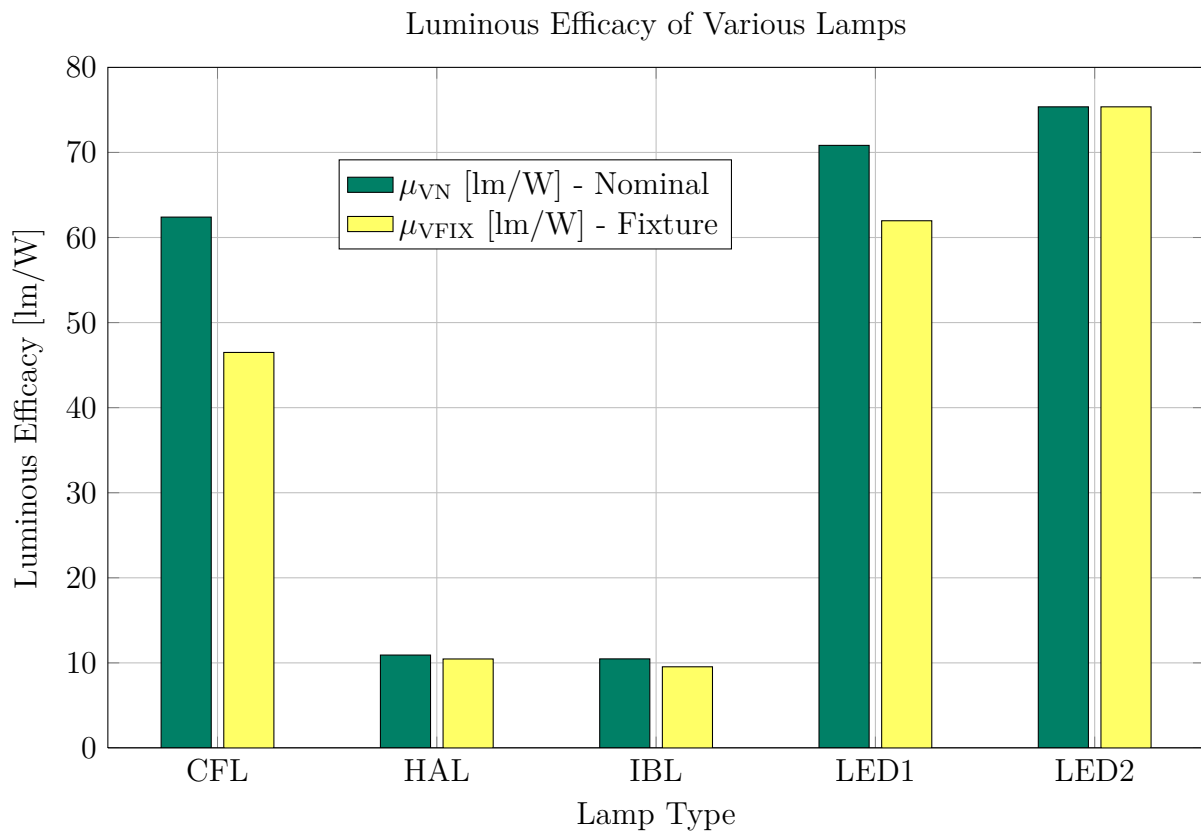


**Figure 7.4:** Lamps efficacy chart.

### 7.1.3 Lamps Polar Diagrams and Conclusions

Some conclusions can be extracted from the obtained results:

- The bigger lamp of all (in volume), has the highest ratio in terms of luminous flux lost in the fixture, followed closely by the LED bulb.
- The halogen lamp has the lowest fixture lumen retention ratio, due to its shape.
- The LED lamp has the highest luminous efficacy of all, but the CFL has good one also.
- The LED lamp has a considerable luminous flux loss in the optical part (6,4%).

The polar diagrams of the various lamps were compared. As expected there were no significant differences between the plane chosen to create the polar diagram, due to the symmetry of the lamps.

However there were a significant difference in the spatial distribution of the LED lamp compared to the remaining ones, as shown in Fig. 7.5.

The polar diagrams for the LED bulb shows a high variable luminous intensity, due to the fact that its interior consists in various discrete light emitters in the form of 12 LEDs.

The polar diagrams of the CFL lamp shows a more uniform spatial distribution of light, due to the inherent light generation method of this lamps, as shown in Fig. 7.6. The incandescent lamp bulb and the halogen one shown similar polar diagrams.

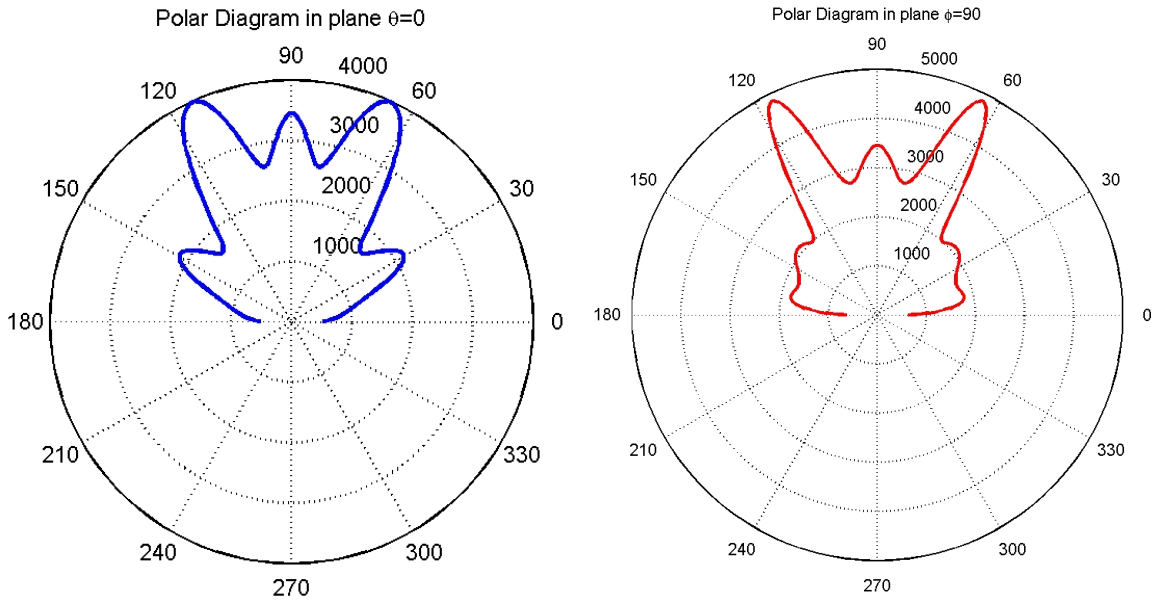


**Figure 7.5:** LED lamp polar diagrams.  
 Left: Polar diagram in plane  $\theta = 0^\circ$ .  
 Right: Polar diagram in plane  $\varphi = 90^\circ$ .

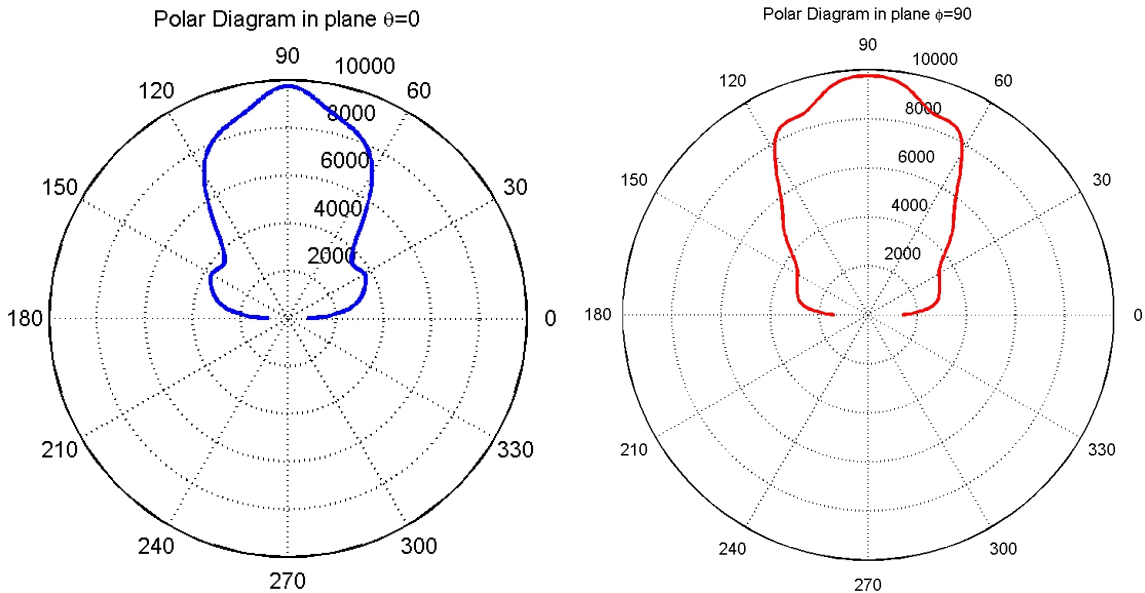


**Figure 7.6:** CFL lamp polar diagrams.  
 Left: Polar diagram in plane  $\theta = 0^\circ$ .  
 Right: Polar diagram in plane  $\varphi = 90^\circ$ .



## 7.2 Drivers Testing

On the laboratory there are 3 LED strings with 9 LEDs each. Using the various strings, and combining them in series or parallel when necessary, will allow to test the power efficiency of the drivers on Table 7.3. The driver of the commercial LED lamp will also be tested and compared against the other drivers.

Brand	Part	$V_{IN}$ [V]	$V_{OUT}$ [V]	$I_{OUT}$ [mA]	$\mu$ [%]	$P_{OUT}$ [W]	Cost [€]
RECOM	RACD60-700	90-264	38-54	700-1100	89	27-60	30
JRDrive	JR-40W	85-265	30-36	1300	>87	40	18

**Table 7.3:** Specifications given by the manufacturers of the drivers available for test.

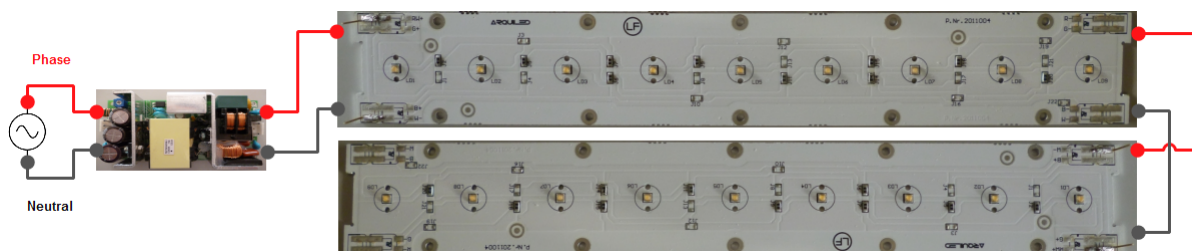


**Figure 7.7:** Configuration for RECOM Driver with 2 strings, with output current at 700 mA.

The Recom driver will be tested with 2 strings in series (Fig. 7.7), so the driver can operate between the input voltage range specified by the manufacturer.

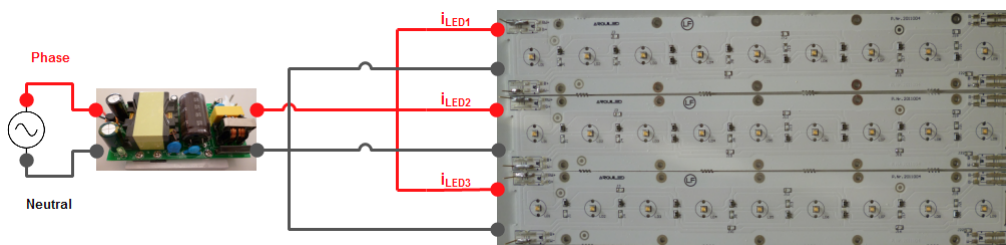


**Figure 7.8:** Configuration for JRLED Driver.

The low cost driver, JRDrive, will be tested with 3 LED strings in parallel (Fig. 7.8), because of its higher current output (1,4A).

### 7.2.1 Driver Testing Results

On Table 7.4, are the results of the driver testing. The data extracted from the RECOM do not allow for conclusions due to the fact that he was not tested with an adequate load. However his efficiency even at half-load is very good.

On the Fig. 7.9, the interior of LED bulb can be seen, exposing the SMD LEDs. Tearing down the lamp completely exposes the driver.

On Fig. 7.10, are shown the LED strings connected to the JRLED driver, with the resulting polar diagrams shown in Fig. 7.11.



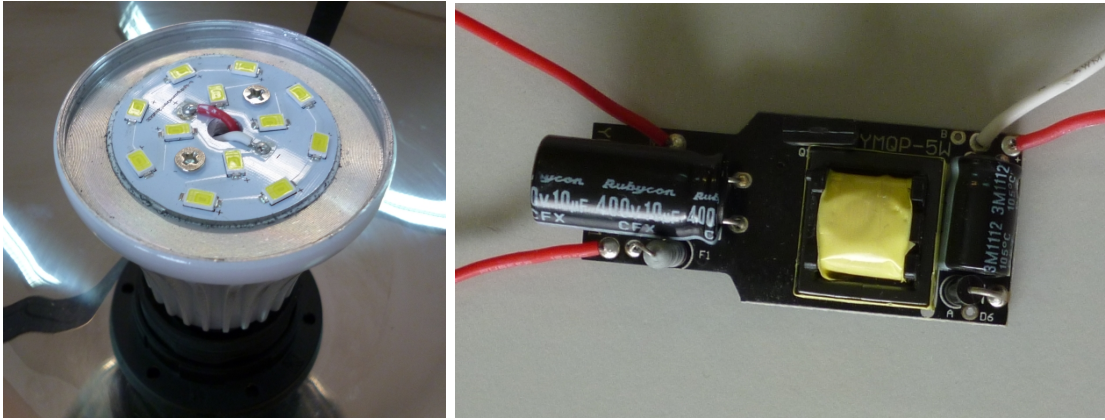


**Figure 7.9:** LED lamp opened.  
 Left: SMD LEDs exposed.  
 Right: Driver.

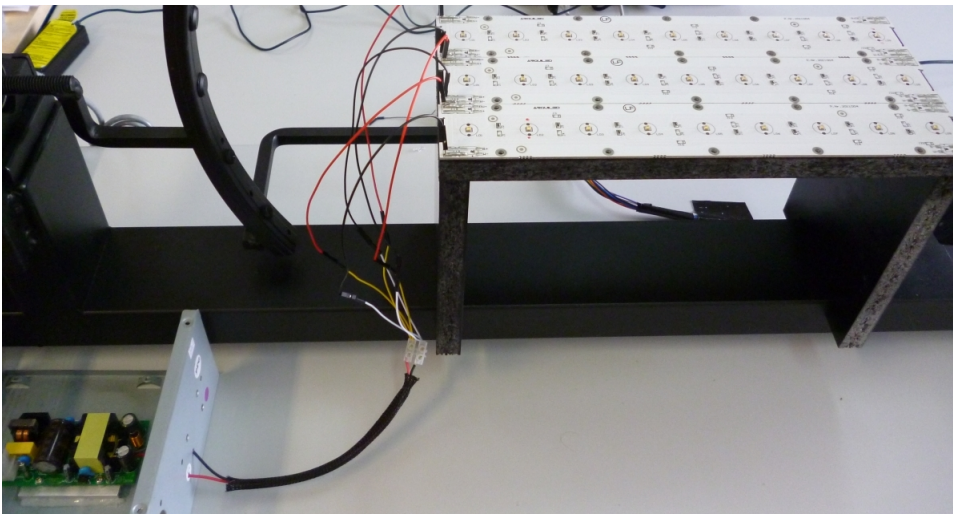


**Figure 7.10:** Setup for the JRLED photometry test.

The LED lamp driver, due to the small size limitations has a modest efficiency. However, as a whole, the lamp driver and the LEDs that come with him deliver a good luminous efficacy, superior to the other 2 setups tested.

### 7.3 LED Light Fixture

From the data acquired in the test two types of charts were created. In the first one, is relative to the luminous efficacy of the source. This is more practical one practical one, since it indicates clearly where are losses, without the technical and difficult task of the luminous

ID	$P_{IN}$ [W]	$P_N$ [W]	$\mu$ [%]	$\Phi_V$ [lm]	$\rho_V$ [lm/W]
RECOM_2str	43,43	38,3	88,2	2862,2	65,9
JRDrive_3str	44,11	37,28	84,5	3296,2	74.72
LAMP_DRV	5,93	4,83	81,4	446,9	75,36

**Table 7.4:** Measurements made to the drivers with the power analyzer.

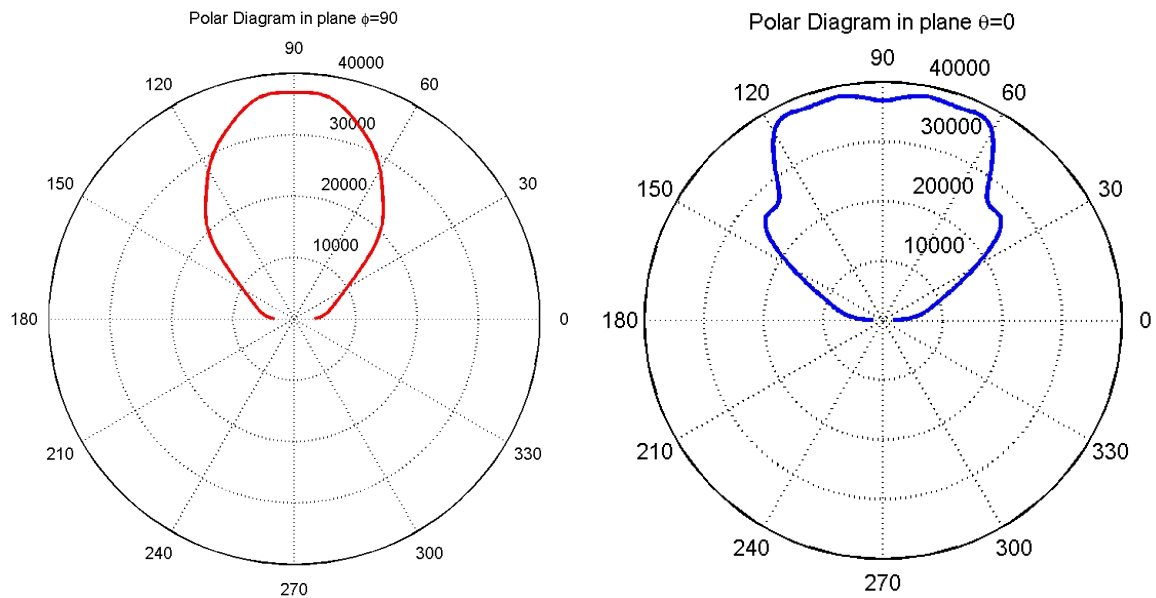


**Figure 7.11:** Polar diagrams of the JRLED test.

Left: Polar diagram in plane  $\theta = 0^\circ$ .

Right: Polar diagram in plane  $\varphi = 90^\circ$ .

coefficient calculation.

The second one indicates the losses in the overall luminous efficacy of a source. Is a more analytical chart to indicate the fact that in the process of creating a polychromatic color, in particular the white one, a great efficiency loss inevitably occur.

### 7.3.1 Luminous Efficacy of Source

On Fig. 7.12, the pie chart shows the losses that occur in the LED lamp placed in the tested fixture. These values certainly differ from other light fixtures, but it can be inferred that the process of converting electrical power into useful luminous power has significant losses along the way.

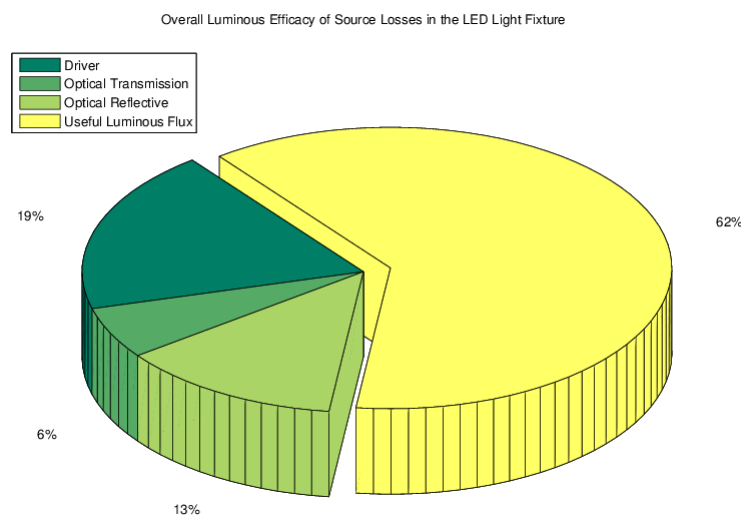


**Figure 7.12:** Luminous efficacy losses of LED Light Fixture

### 7.3.2 Overall Luminous Efficacy of Source

On this efficiency losses chart, was considered a LER efficiency loss (due to the conversion of radiant energy in visible one) of a ideal “white” color. The white LEDs available at the present have a lower LER, although developments are being made to improve it, theoretically passing that ideal white source mark of 27% [58].

The calculations were made with the following efficiency losses in the LED light fixture:

$$\Phi_{MAX} = \Phi_{OUT} \cdot \eta_{RFL} \cdot \eta_{TX} \cdot \eta_{DRV} \cdot V_{COEF}$$

Where  $\Phi_{MAX}$  is the luminous flux obtained from the radiant spectrum with the maximum efficiency, in the case where the spectral distribution consists in monochromatic wavelegh of  $\lambda = 555$  nm. The  $\Phi_{MAX}$  for this particular LED lamp, if the driver was efficiently perfect and the required light was monochromatic green at the wavelength of  $\lambda = 555$  nm, was:

$$\Phi_{MAX} = \frac{446,9}{V_{COEF} \cdot \eta_{DRV}} = 2033 \text{ lm}$$

Then some electrical efficiency occurs in the driver:

$$\Phi_{MAX} \cdot \eta_{DRV} = 549 \cdot 0,814 = 1614 \text{ lm}$$

And, to obtain the white color, a large amount of efficiency is lost (73% considered):

$$\Phi_{MAX} \cdot \eta_{DRV} \cdot V_{COEF} = 2033 \cdot 0,27 = 446,9 \text{ lm}$$

To distribute the light spacially, transmissive optics are required:

$$\Phi_{MAX} \cdot \eta_{DRV} \cdot V_{COEF} \cdot \eta_{TX} = 420 \text{ lm}$$

The reflections in fixture itself causes some efficiency loss, leading after all this process to a small fraction of of the radiant energy converted in visible white luminous flux:

$$\Phi_{MAX} \cdot \eta_{DRV} \cdot V_{COEF} \cdot \eta_{TX} \cdot \eta_{RFL} = 367,5 \text{ lm}$$

On Fig. 7.13, the pie chart shows the luminous total power loss of the LED lamp inserted in light fixture, considering a luminous efficiency of a “ideal white source” (37%).

Many questions still remain about how best to improve the efficiency of LED devices, but it may be unrealistic to assume that the efficiency will be high and constant across all wavelengths, especially when two very different material systems like indium gallium nitride (InGaN) and aluminium gallium indium phosphide (AlInGaP) are used for state of the art HBLEDs.

Given this fact alone, it is doubtful that all LED systems would simultaneously achieve

high color rendering and efficacies  $>200$  lm/W. The most realistic limits would appear to be in the range of 150 to 200 [59, 60].

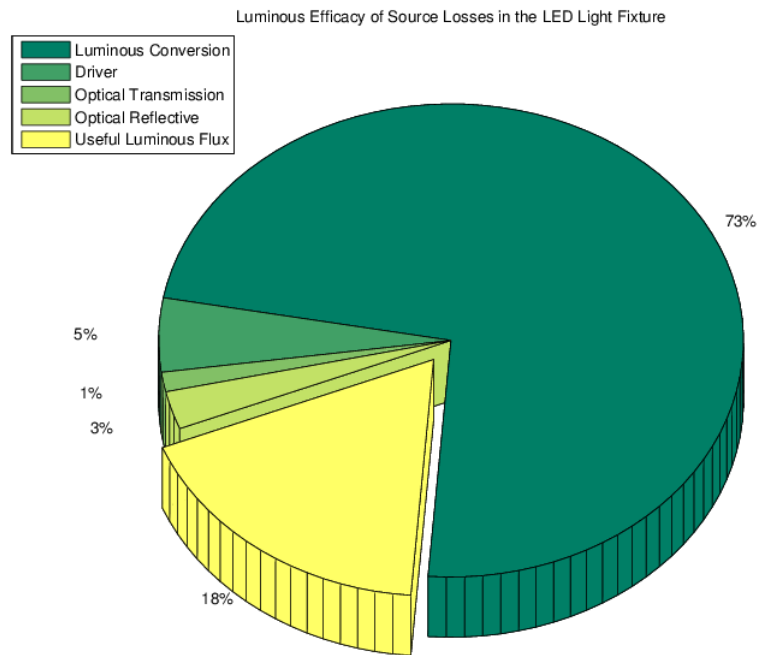


**Figure 7.13:** Luminous total power loss of the LED lamp inserted in light fixture, considering a luminous efficiency of a “ideal white source” (37%).

# Chapter 8

## Conclusions and Future Work

The built goniophotometer measured the total luminous flux and luminous intensity of the various light sources, and those values were presented in the form of polar diagrams.

With the data from the photometry tests, the luminous efficacy of various light sources was calculated and compared. The luminous efficacy of radiation and the radiant efficiency of the source were not taken in account in the luminous efficacy calculation. To obtain  $\eta_E$  and  $\rho_E$ , tests on the light sources using a spectrometer were planned, but due to time constraints, those tests could not be carried on. This topic is of the most importance in LED lighting, specially in the white color, since the increase of the luminous efficacy of radiation is object of ongoing development.

With the fixture used, the magnitude of the losses of the lamps was compared. To obtain a clearer picture of the losses incurring in the fixture, other types of fixtures must be used in a future work, with different shapes and materials.

Although this approach served its purpose, several improvements on this work could be done in order to enrich this kind of project.

The goniophotometer worked as expected although it could be improved in some ways. A possible idea was to create a setup where a light source is rotated against a fixed arc of photodiodes. This way the measurements could be taken at a variable distance.

Other improvements could deal with the error sources and uncertainties. For example, the lux meter used in the calibration has a great uncertainty which limits the accuracy of the results. The photodiodes used on the measurements could be chosen more specifically for visible range detection. Calibration would still be needed, but with less uncertainty, because the sensible spectrum of those photodiodes has a range that approximates the photopic function.

Another base for future work is to investigate how LED light behaves in terms of luminous efficacy in scotopic conditions.

This is an important area of study because of the importance of public lighting quality and cost, where large areas of dim conditions are lit and the human eye responds to scotopic light wavelength range.

# Bibliography

- [1] Peter Apian-bennewitz and Jochen Von Der Hardt. Enhancing and Calibrating a Goniophotometer. *Solar Energy Materials and Solar Cells*, 54(3):309–322, 1998.
- [2] Pietro Fiorentin and Alessandro Scroccaro. Illuminance Standards. *IEEE International Instrumentation and Measurement Technology Conference*, pages 135–140, 2008.
- [3] P. Fiorentin and a. Scroccaro. Analysis of the Performance of a Goniometer for Studying Surface Reflection. *IEEE Transactions on Instrumentation and Measurement*, 57(11): 2522–2527, November 2008. ISSN 0018-9456. doi: 10.1109/TIM.2008.924929. URL <http://ieeexplore.ieee.org/lpdocs/epic03/wrapper.htm?arnumber=4534848>.
- [4] Marcelo Paschoal Dias and Danilo Pereira Pinto Henrique A. C. Braga. A simplified technique of lighting performance evaluation applied to led-based modern luminaires. *2009 Brazilian Power Electronics Conference*, pages 279–284, September 2009. doi: 10.1109/COBEP.2009.5347701. URL <http://ieeexplore.ieee.org/lpdocs/epic03/wrapper.htm?arnumber=5347701>.
- [5] Peter Apian-Bennewitz. New Scanning Goniophotometer for Extended BRDF Measurements. *SPIE Proceedings - Reflection, Scattering, and Diffraction from Surfaces II*, 7792(24):1–20, August 2010. doi: 10.1117/12.860889. URL <http://proceedings.spiedigitallibrary.org/proceeding.aspx?doi=10.1117/12.860889>.
- [6] Tuomas Poikonen, Pasi Manninen, Petri Kärhä, and Erkki Ikonen. Multifunctional Integrating Sphere Setup for Luminous Flux Measurements of Light Emitting Diodes. *The Review of scientific instruments*, 81(2):0231021–023107, February 2010. ISSN 1089-7623. doi: 10.1063/1.3285263. URL <http://www.ncbi.nlm.nih.gov/pubmed/20192480>.
- [7] F Sametoglu. Construction of Two-Axis Goniophotometer for Measurement of Spatial Distribution of a Light Source and Calculation of Luminous Flux. *Acta Physica Polonica A*, 119(6):783–791, 2011.
- [8] Olegs Tetervenoks, Ansis Avotins, and Ilja Galkin. Illumination measurement stand for artificial light sources. *10th international Symposium "Topical Problems in the Field of Electrical and Power Engineering"*, pages 250–254, 2011.
- [9] Hyperphysics. Luminous Efficacy. URL <http://hyperphysics.phy-astr.gsu.edu/hbase/vision/bright.html>.

- [10] PION. Electromagnetic Spectrum. URL <http://www.pion.cz/en/article/electromagnetic-spectrum>.
- [11] Fosilum. Luminous flux in lumens. URL <http://www.fosilum.si/en/zakja-led-svetila/luminous-flux-in-lumens-/>.
- [12] A. A. Gaertner. Optical Radiation Measurement, Modern Metrology Concerns, 2012. URL <http://www.intechopen.com/books/modern-metrology-concerns/optical-radiation-measurements>.
- [13] GAIN11 - The Art & Science of Audio & Video. Inverse Square Law. URL <http://gain11.wordpress.com/2008/06/28/inverse-square-law/>.
- [14] Konica Minolta. Luminance Meters & Colorimeters, 2013. URL <http://sensing.konicaminolta.us/learning-center/light-measurement/luminance-meters-colorimeters/>.
- [15] John Markley. What is Quantum Efficiency?, 2013. URL <http://www.wisegeek.com/what-is-quantum-efficiency.htm>.
- [16] CIE. CIE S 017/E:2011 ILV: International lighting vocabulary, new, 2011.
- [17] Craig DiLouie. Evaluating the Efficiency of Light Fixtures, 2010. URL [www.nalmco.org/WorkArea/DownloadAsset.aspx/.../Summer2010\\_DeLouieArticle.pdf](http://www.nalmco.org/WorkArea/DownloadAsset.aspx/.../Summer2010_DeLouieArticle.pdf).
- [18] Nathan Moroney, Mark D Fairchild, Robert W G Hunt, Changjun Li, M Ronnier Luo, and Todd Newman. The CIECAM02 Color Appearance Model. pages 23–27.
- [19] E-Lite OptoTech. CRI. URL <http://www.elite-opto.com/tech/2012-04-27-16-59-5865.html>.
- [20] Full Spectrum Solutions. CRI Explained. URL [http://www.fullspectrum solutions.com/cri\\_explained.htm](http://www.fullspectrum solutions.com/cri_explained.htm).
- [21] Rudiger Paschotta. Integrating Spheres. URL [http://www.rp-photonics.com/integrating\\_spheres.html](http://www.rp-photonics.com/integrating_spheres.html).
- [22] Labsphere. MtrX-SPEC Software from Labsphere Transitions from R&D to Production, 2008. URL <http://halmapr.com/news/labsphere/category/product-news/page/3/>.
- [23] J. Hodgkinson. Open Optics, 2012. URL <http://openoptics.info/blog/2012/12/21/an-inside-out-snowman/>.
- [24] STIL SA. REFLET Goniophotometer. URL [http://www.stilsa.com/EN/prod/reflet/reflet\\_scat.htm](http://www.stilsa.com/EN/prod/reflet/reflet_scat.htm).



- [25] Instrument Systems - Optronik Division. Goniophotometers. URL <http://www.optronik.de/plm-goniophotometers.shtml>.
- [26] Ligman Lighting. Photometric Laboratory, 2012. URL <http://www.ligmanlighting.com/fi/lighting-laboratory/lighting-laboratory>.
- [27] DIN. 5032-7:1985 Photometry; Classification of illuminance Meters and Luminance Meters. Technical report, 1985.
- [28] CIE. Publication No. 69 - Methods of Characterizing Illuminance Meters and Luminance Meters: Performance, Characteristics and Specifications. Technical report, 1987.
- [29] BSI. British Standard, BS 667:2005 Illuminance Meters - Requirements and Test methods. Technical report, 2005.
- [30] P.R. Boyce. *Philips Lighting Manual - Third Edition*. Sage Publications, 1982.
- [31] IEC. 60598-1 - Luminaires - General Requirements and tests. Technical report, 2006.
- [32] Aramando Roggio. Thermal Management is Key for LED Luminaire Design. URL <http://www.digikey.com/us/en/techzone/lighting/resources/articles/LED-Luminaire-Design.html>.
- [33] OSRAM. LED luminaires: energy-efficient, stylish lighting solutions. URL [http://www.osram.com/osram\\_com/trends-and-knowledge/led-home/professional-knowledge/technologies/led-luminaires/index.jsp](http://www.osram.com/osram_com/trends-and-knowledge/led-home/professional-knowledge/technologies/led-luminaires/index.jsp).
- [34] JPSA Advanced Laser Technology. LED Primer. URL [http://www.jpسالaser.com/apps\\_led.html](http://www.jpسالaser.com/apps_led.html).
- [35] Nibedita Das. Studies on Low Cost LED Based Solar Cell for Emergency Lighting. *International Journal of Engineering Sciences & Research Technology*, 2(2), 2013.
- [36] Premiere Lighting. LED Lighting, 2013. URL <http://www.premierltg.com/led-lighting/>.
- [37] Aalto University. Lighting Technologies. URL [http://www.lightinglab.fi/IEAAnnex45/guidebook/5\\_lightingtechnologies.pdf](http://www.lightinglab.fi/IEAAnnex45/guidebook/5_lightingtechnologies.pdf).
- [38] Thomas W. Murphy. Maximum spectral luminous efficacy of white light. *Journal of Applied Physics*, 111(10):6, 2012. URL [http://jap.aip.org/resource/1/japiau/v111/i10/p104909\\_s1?isAuthorized=no](http://jap.aip.org/resource/1/japiau/v111/i10/p104909_s1?isAuthorized=no).
- [39] Lighting Research Center. How is white light made with LEDs?, 2003. URL <http://www.lrc.rpi.edu/programs/nlpip/lightinganswers/led/whiteLight.asp>.



- [40] Navigant Consulting. Solid-State Lighting Research and Development, 2009. URL [http://apps1.eere.energy.gov/buildings/publications/pdfs/ssl/ssl\\_mypp2009\\_sec4.pdf](http://apps1.eere.energy.gov/buildings/publications/pdfs/ssl/ssl_mypp2009_sec4.pdf).
- [41] Wikipedia. Wien's displacement law, . URL [http://en.wikipedia.org/wiki/Wien's\\_displacement\\_law](http://en.wikipedia.org/wiki/Wien's_displacement_law).
- [42] LEDs Magazine. Avoiding thermal runaway when driving multiple LED strings, 2009. URL <http://ledsmagazine.com/features/6/2/2>.
- [43] Jaycar Electronics. DC-DC Converters : A Primer. Technical Report 1, 2001.
- [44] Microchip Technology Incorporated, All Rights Reserved, and Smmps Components. SMPS Components and their effects on System Design. pages 1–31, 2006.
- [45] Mark Gebbia. Low ESR Capacitors: Fact or Fiction? URL [http://www.illinoiscapacitor.com/pdf/Papers/low\\_ESR\\_fact\\_or\\_fiction.pdf](http://www.illinoiscapacitor.com/pdf/Papers/low_ESR_fact_or_fiction.pdf).
- [46] CandlePowerForumns. High Power LED. URL <http://www.candlepowerforums.com/vb/showthread.php?357925-High-Power-LED&p=4167484>.
- [47] CREE. LED Luminaire Design Guide, 2012. URL [http://www.cree.com/~media/Files/Cree/LEDComponentsandModules/XLamp/XLampApplicationNotes/LED\\_Luminaire\\_Design\\_Guide.pdf](http://www.cree.com/~media/Files/Cree/LEDComponentsandModules/XLamp/XLampApplicationNotes/LED_Luminaire_Design_Guide.pdf).
- [48] My LED Lighting Guide. Better Vision with LED lights - Scotopic and Photopic Vision, 2011. URL <http://www.myledlightingguide.com/WhitePapers/WhitePaperLEDlightandScotopicLumens.pdf>.
- [49] IES. Measuring Lumen Maintenance of LED Sources. Technical report, 2008.
- [50] Marc Dyble. Methods of Achieving High CRI with LEDs. URL <http://pl.mouser.com/applications/lighting-cri/>.
- [51] Vishay Semiconductors. Measurement Techniques, 2012. URL <http://www.vishay.com/docs/80085/measuram.pdf>.
- [52] Vishay. Silicon PIN Photodiode, 2011. URL <http://www.vishay.com/docs/81521/bpw34.pdf>.
- [53] Richard Sear. Thermal Johnson-Nyquist effect. URL <http://marie.ph.surrey.ac.uk/~phs1rs/teaching/nyquist.pdf>.
- [54] LED Museum. Spectra of LEDs. URL <http://ledmuseum.candlepower.us/led/spectra6.htm>.
- [55] IKATECH. Lighting Terminology. URL [http://www.ikatech.net/index.aspx?lang=eng&fn=technical\\_language](http://www.ikatech.net/index.aspx?lang=eng&fn=technical_language).

- [56] Wikipedia. Photodiode, . URL <http://en.wikipedia.org/wiki/Photodiode>.
- [57] Andrew Olson. How Does Color Affect Heating by Absorption of Light?, 2013. URL [http://www.sciencebuddies.org/science-fair-projects/project\\_ideas/Phys\\_p030.shtml](http://www.sciencebuddies.org/science-fair-projects/project_ideas/Phys_p030.shtml).
- [58] Guoxing He, Lihong Zheng, and Huafeng Yan. LED white lights with high CRI and high luminous efficacy. *SPIE Proceedings*, 7852, 2010.
- [59] Electronics Point. Theoretical efficacy limit for LED. URL <http://www.electronicspoint.com/theoretical-efficacy-limit-led-t222379.html>.
- [60] Eric Bretschneider. Efficacy Limits for Solid-State White Light Sources. URL <http://www.photonics.com/Article.aspx?AID=28677>.

# Appendix A

## Goniophotometer Construction and Operation

The materials employed on the construction of the goniometer were choosed keeping in mind it's low cost and ease of assembly, so the decision to employ a bicycle rim came naturally, because the equidistant spaces between the spokes. Also the rim have a exterior surface that can be used to connect all the necessary wires in a convenient way, non obstructing the path of the luminous flux.

The rim is fixed to a metallic sub-structure, with roller bearings conecting the rotating axis to the rotary positioner. The whole main structure was designed in such a way that it would be symmetric for simplicity and ease of construction, and ensuring a user friendly assembly and operation, whilst allowing room for the wires and not interfering with the light flux.

After the completion of the structure, a black paint was given to minimize the light reflections.

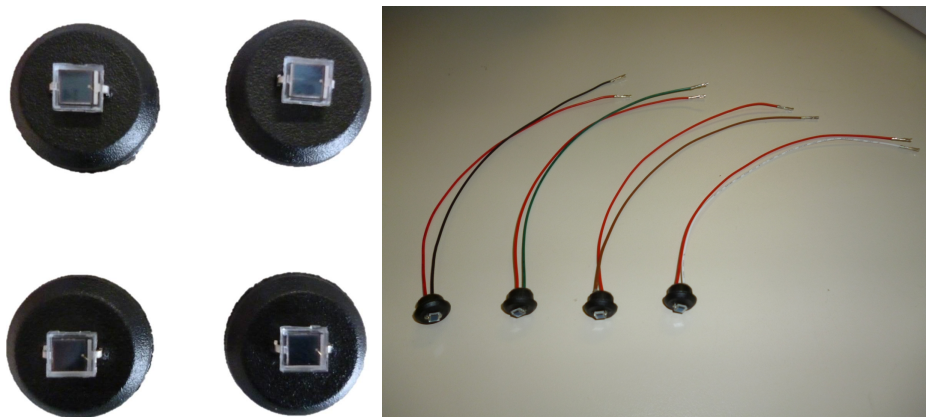


**Figure A.1:** Photodiodes incorporation on arc.

Left: Top view of the photodiodes inserted on rubber, to fit in the rim holes.

Right: Photodiodes connected to cables.

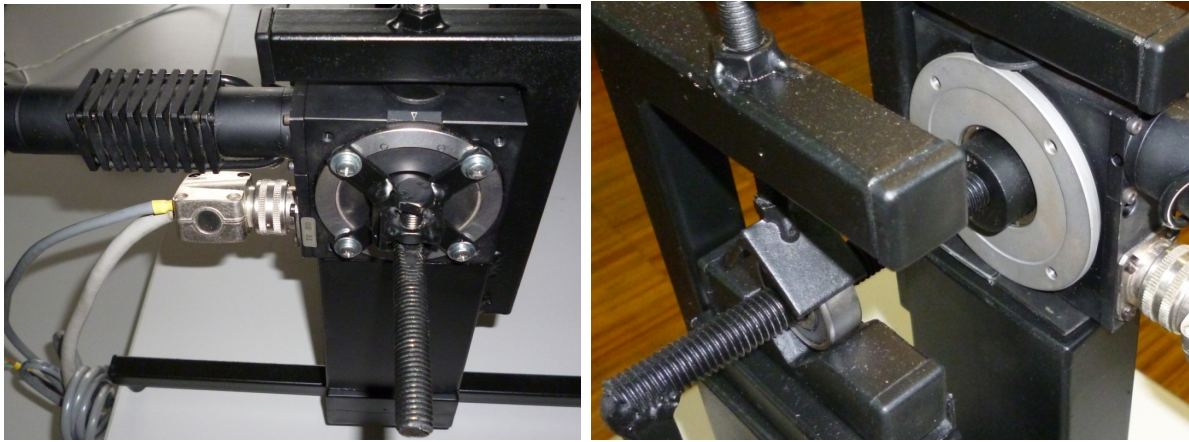


**Figure A.2:** Rotary positioner stage.  
Left: External view.  
Right: Internal view.



**Figure A.3:** Goniophotometer after completion.

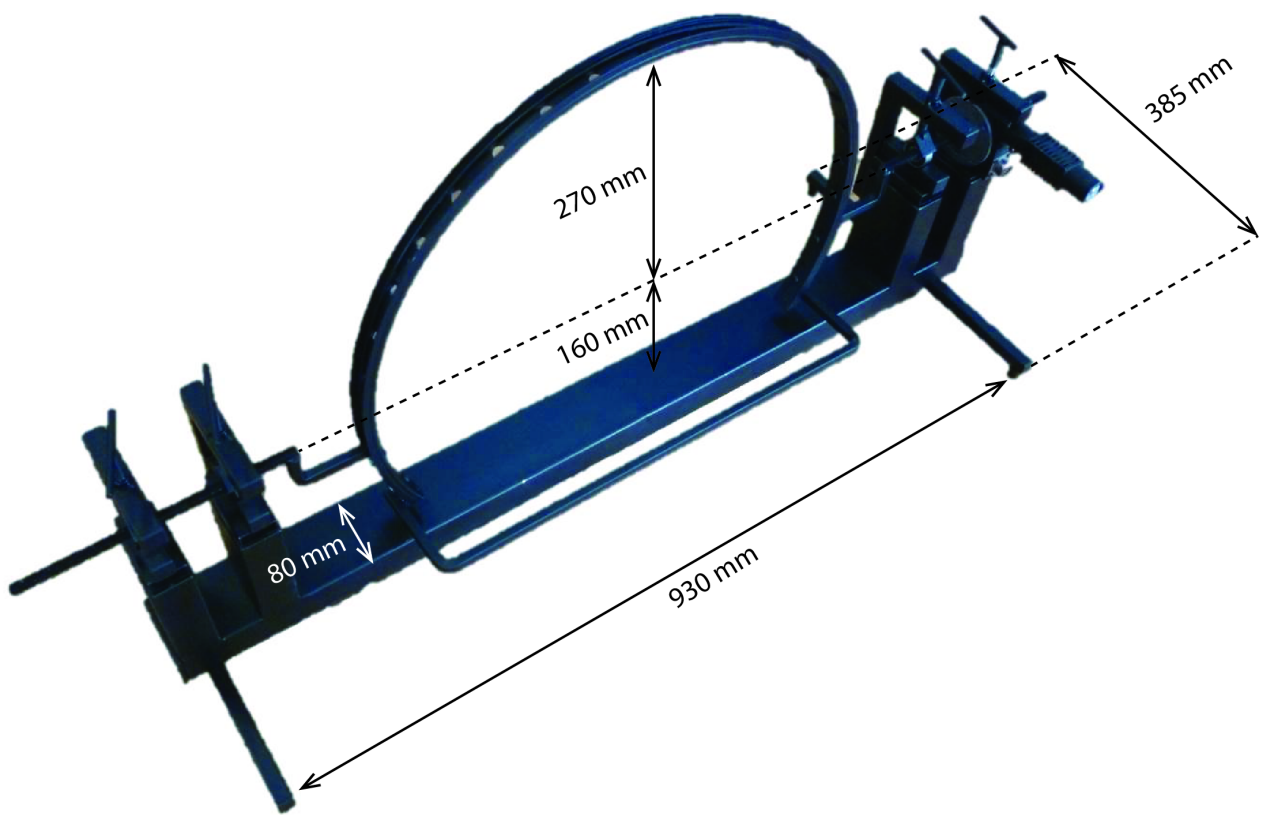


**Figure A.4:** Goniophotometer dimensions.

## A.1 Code developed to operate the Goniophotometer in MATLAB

```

1  % Bruno Lopes
2  % ISR
3  % March 2013
4  %% Script to calculate the total luminous flux and polar diagrams
5  delete(instrfindall);
6  clear all ,close all,clc
7  format shortg
8  scrsz=get(0,'Screensize');
9  scrsz(2) = 50;
10 scrsz(4) = scrsz(4)-150;
11 %% Variable Initialization
12 % Arc radius [meters]
13 % Some tolerance must be given to the radius because of the rubber
14 % in wich the photodiodes will fit.
15 Tolerance=0.006;
16 r=0.27-0.006;
17 % Photodiode positions in spherical coordinates phi [degrees]
18 phi=[180 170 160 150 140 130 120 110 100 90];
19 % Shunt Resistor [ohms]
20 R=8450;
21 % Wanted slices of a sphere quadrant
22 % Step size [degrees]=90/slices
23 slices=10;
24 % Relation between the Photodiode reverse current [A]
25 % and the Illuminance [lx]
26 K=(1/0.075)*1e6;
27 % Check previously the serial port attribution of CAN Adapter
28 serial_CAN = 'COM5';
29 % Check previously the serial port attribution of Arduino Mega
30 serial_arduino = init_arduino('COM7');
31 % Wait time after step step_time=2.5;
32 % Number of samples to aquire in each step
33 n_samples = 50;
34 % Calibration scalar due to the photodiodes spectral range
35 C=5;
36 %% Rotary Positioner initialization
37 % Axis ID axis_id = 1;
38 % CANopen bus global variables
39 global can_frames;
40 global can_frames_index;
41 global debug_can_bus;
42 global canusb;
43 % Internal units conversion
44 global degree_to_IU;
45 global degree_s_to_IU;

```



```

46 global degree_s2_to_IU;
47 global sec_to_IU;
48 can_frames = [];
49 can_frames_index = 1;
50 % 1 to debug CAN msgs, 0 for debug OFF
51 debug_can_bus = 1;
52 % 1 for CANSUB, 0 for EasySync
53 canusb = 0;
54 disp('Micro-Controle Calib - Setting up IU conversion rates...')
55 no_usteps = 256; % Number of micro-steps p/ step
56 no_steps = 200; % Number of steps p/ revolution
57 Tr = 2*pi*5; % Relation between motor and load
58 T = 0.0008; % The slow loop sampling period expressed in (s)
59 degree_to_IU = 2*pi/(no_usteps*no_steps*Tr);
60 degree_s_to_IU = 2*pi/(no_usteps*no_steps*Tr*T);
61 degree_s2_to_IU = 2*pi/(no_usteps*no_steps*Tr*T*T);
62 sec_to_IU = T;
63 disp(['Micro-Controle Calib - Opening serial port ' port_name '...']);
64 % Serial port settings
65 serial_port = serial(port_name);
66 set(serial_port, 'BaudRate', 115200);
67 set(serial_port, 'BytesAvailableFcn', @CANbusCallback);
68 set(serial_port, 'BytesAvailableFcnMode', 'terminator');
69 set(serial_port, 'Terminator', 13);
70 % Open the serial port
71 fopen(serial_port);
72 pause(0.5);
73 % Open the CAN channel
74 openCANChannel(serial_port);
75 pause(0.5);
76 disp('Micro-Controle Calib - Initializing Technosoft Drive...');
77 % Initialize the Technosoft IDM680-8EI drive initializeTechnosoftDrive(
    serial_port);
78 disp('Micro-Controle Calib - Initializing Technosoft Drive... [DONE]');
79 disp('Micro-Controle Calib - Running the main loop...');
80 setupPositionMode(serial_port, 1.0, 1.0);
81 pause(0.5)
82 %% Data Aquisition with Arduino Mega
83 pause(2)
84 % Data sample test
85 data = read_arduino(serial_arduino)
86 % 10 Photodiodes will be used
87 output_ph1 = [];
88 output_ph2 = [];
89 output_ph3 = [];
90 output_ph4 = [];
91 output_ph5 = [];
92 output_ph6 = [];
93 output_ph7 = [];

```

```

94 output_ph8 = [];
95 output_ph9 = [];
96 output_ph10 = [];
97 % Interval between aquisitions [degrees]
98 step = 90/slices;
99 % Aquisition number equal to interval size plus initial and final
   positions
100 aquisitions = step+2;
101 for i=1 : aquisitions
102     line_ch1 = [(i-1)*step];
103     line_ch2 = [(i-1)*step];
104     line_ch3 = [(i-1)*step];
105     line_ch4 = [(i-1)*step];
106     line_ch5 = [(i-1)*step];
107     line_ch6 = [(i-1)*step];
108     line_ch7 = [(i-1)*step];
109     line_ch8 = [(i-1)*step];
110     line_ch9 = [(i-1)*step];
111     line_ch10 = [(i-1)*step];
112     pause(step_time)
113     for j=1 : number_of_samples
114         try
115             data = read_arduino(serial_arduino);
116         catch exception_data
117             pause(1)
118             disp('In exception');
119         try
120             data = read_arduino(serial_arduino);
121         catch exception_data2
122             pause(1)
123             disp('In exception2');
124             data = read_arduino(serial_arduino);
125     end
126     end
127     line_ch1 = [line_ch1 data(1)];
128     line_ch2 = [line_ch2 data(2)];
129     line_ch3 = [line_ch3 data(3)];
130     line_ch4 = [line_ch4 data(4)];
131     line_ch5 = [line_ch5 data(5)];
132     line_ch6 = [line_ch6 data(6)];
133     line_ch7 = [line_ch7 data(7)];
134     line_ch8 = [line_ch8 data(8)];
135     line_ch9 = [line_ch9 data(9)];
136     line_ch10 = [line_ch10 data(10)];
137     end
138     pause(step_time)
139     output_ph1 = [output_ph1 ; line_ch1];
140     output_ph2 = [output_ph2 ; line_ch2];
141     output_ph3 = [output_ph3 ; line_ch3];

```



```

142     output_ph4 = [output_ph4 ; line_ch4];
143     output_ph5 = [output_ph5 ; line_ch5];
144     output_ph6 = [output_ph6 ; line_ch6];
145     output_ph7 = [output_ph7 ; line_ch7];
146     output_ph8 = [output_ph8 ; line_ch8];
147     output_ph9 = [output_ph9 ; line_ch9];
148     output_ph10 = [output_ph10 ; line_ch10];
149     if i < aquisitions
150         sendMotorToPosition_degree(serial_port , i*step);
151         run(serial_port);
152         waitForGoal(serial_port , 3.0);
153     end
154 end
155 % Close ADC channels
156 delete(serial_arduino);
157 clear serial_arduino;
158 % Go to homing position
159 go2degree(serial_port , 0 )
160 disp('Micro-Controle Calib - Running the main loop... [DONE]');
161 %% Data Treatment
162 AUX1=output_ph1(:,2:end);
163 AUX2=output_ph2(:,2:end);
164 AUX3=output_ph3(:,2:end);
165 AUX4=output_ph4(:,2:end);
166 AUX5=output_ph5(:,2:end);
167 AUX6=output_ph6(:,2:end);
168 AUX7=output_ph7(:,2:end);
169 AUX8=output_ph8(:,2:end);
170 AUX9=output_ph9(:,2:end);
171 AUX10=output_ph10(:,2:end);
172 PH1=mean(AUX1 ,2)
173 PH2=mean(AUX2 ,2)
174 PH3=mean(AUX3 ,2)
175 PH4=mean(AUX4 ,2)
176 PH5=mean(AUX5 ,2)
177 PH6=mean(AUX6 ,2)
178 PH7=mean(AUX7 ,2)
179 PH8=mean(AUX8 ,2)
180 PH9=mean(AUX9 ,2)
181 PH10=mean(AUX10 ,2)
182 photodiodes=[PH10 ' ; PH9 ' ; PH8 ' ; PH7 ' ; PH6 ' ; PH5 ' ; PH4 ' ; PH3 ' ; PH2 ' ; PH1 ' ];
183     illuminance=photodiodes.*(K/R)*C;
184 [X,Z,Y] = sphere(40);
185 X= X(1:21,1:11);
186 Y=-Y(1:21,1:11);
187 Z=-Z(1:21,1:11);
188 % Insert 19 photodiodes from 0 to 180° [phi]
189 for i=1:11 xi(:,i)=interp1(linspace(0,1,21),X(:,i),linspace(0,1,10),'
    spline'); yi(:,i)=interp1(linspace(0,1,21),Y(:,i),linspace(0,1,10),'

```

```

    spline'); zi(:,i)=interp1(linspace(0,1,21),Z(:,i),linspace(0,1,10),'
    spline');
189 end
190 % Time the radius of Photodiodes
191 xi=xi*r;
192 yi=yi*r;
193 zi=zi*r;
194 % http://geomalgorithms.com/a01-\_area.html
195 for i=1:10
196 V0=[xi(1,i) yi(1,i) zi(1,i)];
197 V1=[xi(2,i) yi(2,i) zi(2,i)];
198 V2=[xi(2,i+1) yi(2,i+1) zi(2,i+1)];
199 V3=[xi(1,i+1) yi(1,i+1) zi(1,i+1)];
200 areas(i)=sum(cross((V2-V0),(V3-V1)))*4/2;
201 end
202 areas= repmat(areas,10,1);
203 % 4 quadrants
204 TOTAL=sum(sum(areas.*illuminance(:,2:end)))*4;
205 [X,Z,Y] = sphere(40);
206 X= X(1:41,1:21);
207 Y=-Y(1:41,1:21);
208 Z=-Z(1:41,1:21);
209 % Insert 19 photodiodes from 0 to 180° [phi]
210 for i=1:21
211 xi2(:,i)=interp1(linspace(0,1,41),X(:,i),linspace(0,1,19),'spline');
    yi2(:,i)=interp1(linspace(0,1,41),Y(:,i),linspace(0,1,19),'spline');
    zi2(:,i)=interp1(linspace(0,1,41),Z(:,i),linspace(0,1,19),'spline');
212 end
213 % Times
214 xi2=xi2*r;
215 yi2=yi2*r;
216 zi2=zi2*r;
217 figure('Name','Aquired illuminances','NumberTitle','off');
218 surf(xi2,yi2,zi2)
219 daspect([1 1 1])
220 view(80, 20);
221 title('Aquired illuminances')
222 xlabel('X axis - Photodiodes');
223 ylabel('Y axis - Steps');
224 zlabel('Z axis');
225 %% Polar Diagrams
226 figure('Name','Polar Diagram in plane theta=0','NumberTitle','off'); aux
    =[illuminance(end:-1:2,1),illuminance(:,1)']; rho=interp1(linspace
    (0,1,length(aux)),aux(:),linspace(0,1,361),'spline'); theta=deg2rad
    (0:0.5:180);
227 polar(theta,rho); title('Polar Diagram in plane \theta=0')
228 figure('Name','Polar Diagram in plane \phi=90','NumberTitle','off'); aux
    =[illuminance(1,end:-1:2),illuminance(1,:)']; rho2=interp1(linspace
    (0,1,length(aux)),aux(:),linspace(0,1,361),'spline'); theta2=deg2rad

```

```
(0:0.5:180);  
229 polar(theta2,rho2);  
230 title('Polar Diagram in plane \phi=90')  
231 end
```

## A.2 Graphic User Interface

A graphic user interface was made integrating a useful set of options to control the goniophotometer:

- The interface allows the the aquisition of new measurements or data loading of previously made scannings;
- The polar diagram can be displayed for  $\varphi = 90^\circ$  and for  $\theta = 0^\circ$ ;
- The discretization level is choosed by the number of slices (this number refers to the whole hemisphere);
- Several calibration profiles can be selected;
- If the photodiodes are replaced, the new relation between reverse current and illuminance can be inserted;
- At the start is displayed the fixed COM port attributions so the user knows if a new attribution is necessary;
- The value of shunt resistor can be modified, as the pause duration between steps and the number of samples aquired in each discretization along  $\theta$ .

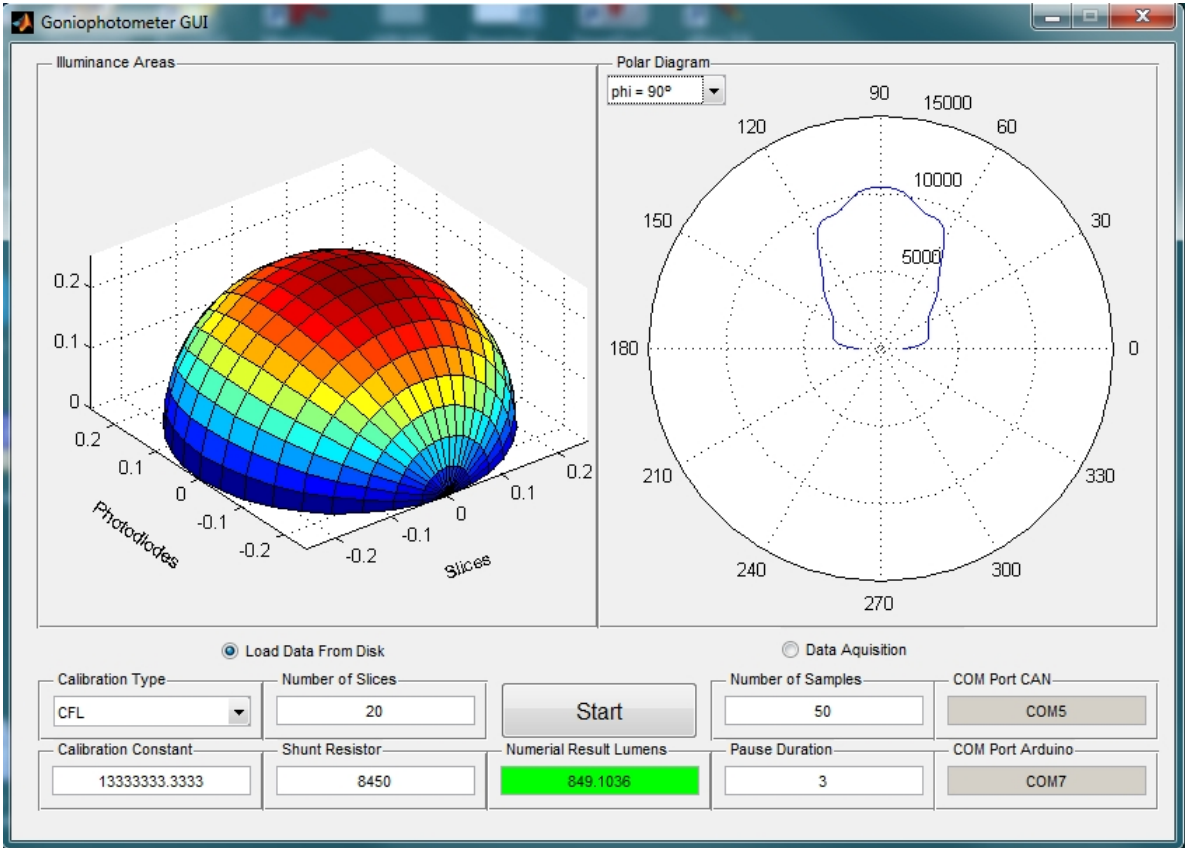


Figure A.5: Developed GUI for the goniophotometer.

# Appendix B

## Integrating Sphere Theory

Deriving the radiance of an internally illuminated integrating sphere begins with an expression of the radiance,  $L$ , of a diffuse surface for an input flux,  $\Phi_I$ .

$$L = \frac{\Phi_I \rho}{\pi A} \quad (\text{A.1})$$

The radiance  $L$ , is expressed in  $\text{W} \cdot \text{m}^{-2} \cdot \text{sr}^{-1}$  where  $\rho$  is the reflectance,  $A$  the illuminated area and  $\pi$  the total projected solid angle from the surface.

For an integrating sphere, the radiance equation must consider both multiple surface reflections and losses through the port openings needed to admit the input flux,  $\Phi_I$ , as well as view the resulting radiance. Consider a sphere with input port area  $A_I$  and exit port  $A_E$ .

The input flux is perfectly diffused by the initial reflection. The amount of flux incident on the entire sphere surface is:

$$\Phi_1 = \Phi_I \rho \left( \frac{A_S - A_I - A_E}{A_S} \right) \quad (\text{A.2})$$

Where the quantity in parenthesis denotes the fraction of flux received by the sphere surface that is not consumed by the port openings. It is more convenient to write this term as  $(1 - f)$  where  $f$  is the port fraction and  $f = \frac{(A_I + A_E)}{A_S}$ . When more than two ports exist,  $f$  is calculated from the sum of all port areas.

By similar reasoning, the amount of flux incident on the sphere surface after the second reflection is:

$$\Phi_2 = \Phi_I \rho^2 (1 - f)^2 \quad (\text{A.3})$$

The third reflexion produces an amount of flux equal to

$$\Phi_3 = \Phi_I \rho^3 (1 - f)^3 \quad (\text{A.4})$$

It follows that after  $n$  reflexions, the total flux incident over the entire integrating sphere surface is:

$$\Phi_I \rho (1 - f) \left\{ 1 + \rho (1 - f) + \dots + \rho^{n-1} (1 - f)^{n-1} \right\} \quad (\text{A.5})$$

Expanding to an infinite power series, and given that  $r(1 - f) < 1$ , this reduces to a simpler form:

$$\Phi_n = \frac{\Phi_I \rho (1 - f)}{1 - \rho (1 - f)} \quad (\text{A.6})$$

Equation indicates that the total flux incident on the sphere is higher than the input due to multiple reflections inside the cavity. It follows that the sphere surface radiance is given by:

$$L_S = \frac{\Phi_I}{\pi A_S (1 - f)} \cdot \frac{\rho (1 - f)}{1 - \rho (1 - f)} = \frac{\Phi_I}{\pi A_S} \cdot \frac{\rho}{1 - \rho (1 - f)} \quad (\text{A.7})$$

This equation is used to predict integrating sphere radiance for a given input flux as a function of sphere diameter, reflectance, and port fraction. Note that the radiance decreases as sphere diameter increases

Equation 2.7 is purposely divided into two parts. The first part is approximately equal to equation A.1, the radiance of a diffuse surface. The second part of the equation is a unitless quantity which can be referred to as the sphere multiplier.

$$M = \frac{\rho}{1 - \rho (1 - f)} \quad (\text{A.8})$$

It accounts for the increase in radiance due to multiple reflections. The following chart illustrates the magnitude of the sphere multiplier,  $M$ , and its strong dependence on both the port fraction,  $f$ , and the sphere surface reflectance  $r$ .

The sphere multiplier in equation A.8 is specific to the case where the incident flux impinges on the sphere wall, the wall reflectance is uniform and the reflectance of all port areas is zero. The general expression is:

$$M = \frac{\rho_0}{1 - \rho_W (1 - \sum_{i=0}^n f_i) - \sum_{i=0}^n \rho_i f_i} \quad (\text{A.9})$$

where

$\rho_0$  = the initial reflectance for incident flux

$\rho_W$  = the reflectance of the sphere wall

$\rho_i$  = the reflectance of port opening  $i$

$f_i$  = the fractional port area of port opening  $i$

The quantity can also be described as the average reflectance  $\bar{\rho}$  for the entire integration sphere. Therefore, the sphere multiplier can be rewritten in terms of both the initial and average reflectance:

$$M = \frac{\rho_0}{1 - \bar{\rho}} \quad (\text{A.10})$$

An exact analysis of the distribution of radiance inside an actual integrating sphere would depend on the distribution of incident flux, the geometrical details of the actual sphere design, and the reflectance distribution function for the sphere coating as well as each surface of each device mounted at a port opening or inside the integrating sphere. Design guidelines for optimum spatial performance are based on maximizing both the coating reflectance and the sphere diameter with respect to the required port openings and system devices. The effect of the reflectance and port fraction on the spatial integration can be illustrated by considering the number of reflections required to achieve the total flux incident on the sphere surface given by equation A.6. The total flux on the sphere wall after only  $n$  reflections can be written as:

$$\Phi_n = \Phi_I \sum_{n=1}^n \rho^n (1 - f)^n \quad (\text{A.11})$$

# Appendix C

## Relevant Standards for LED Light

C.1 Performance

C.2 Electromagnetic Compability

C.3 Funcionality

C.4 Security

Standard	Date	Description
IEC	2111	LED Module for General Lighting - Performance
IEC/EN 62384 +A1	2006	DC or AC supplied electronic control gear for LED modules - Performance requirements
IEC/TR 61341 ed.2	2111	Method of measurement of centre beam intensity and beam angle (s) of reflector lamps
Pr. IEC 62612	2011	Self-ballasted LED-lamps for general lighting services > 50 V - Performance requirements: doc 34A/1343/CDV

**Table C.1:** Standards related to performance



Standard	Year	Description
EN 55015	2111	Radio disturbances characteristics
IEC/EN 61000-3-2	2111	Limits for harmonic current emissions
IEC/EN 61000-3-3	2111	Limitations of voltage changes, voltage fluctuations and flicker
IEC/EN 61547	2111	Immunity requirements

**Table C.2:** Standards related to EMC

Standard	Year	Description
IEC 62386-207		Digital adressable lighting interface-Part 207: Particular requirements for control gears; LED modules (device type 6)
IEC/EN 60061		Lamp Caps and holders
IEC/EN 60598	2004	Luminaire Requirements
IEC/EN 60838-2-2		Connectors for LED-modules

**Table C.3:** Standards related to functionality

Standard	Year	Description
IEC 61231		International lamp coding system (ILCOS)
IEC/TS 62504		Terms and definitions for LEDs and LED modules in general lighting:34A/1355/DTS
EN 62471:2008		Photobiological safety of lamps and lamp systems (see Annex A to Guide)
IEC TR 62471-2		Photobiological safety of lamps and lamp systems - Part 2: guidance on manufacturing requirements relating to non-laser optical radiation safety (see Annex A to the guide)
IEC/EN 60825-1		Safety for laser products (see Annex A)
IEC/EN 61347-1		Lamp control gear - Part 1: General and safety requirements
IEC/EN 61347-2-13		Lamp control gear - Part 2-13: Particular requirements for d.c. or a.c. supplied electronics controlgear for LED General and safety requirements
IEC/EN 62031		LED Modules for General Lighting - Safety Specifications
Pr. IEC 62560		Self-ballasted LED-lamps for general lighting services by voltage >50 V - Safety specifications: doc 34A/1354/CDV

**Table C.4:** Standards related to security